A review of alkaline electrolyzer technology modeling and applications for decision-making optimization in energy systems

Huang, Chunjun; Torres, José Luis Rueda; Zong, Yi; You, Shi; Jin, Xin

DOI
10.1016/j.rser.2025.116005

Publication date
2025

Document Version
Final published version

Published in
Renewable and Sustainable Energy Reviews

Renewable and Sustainable Energy Reviews 224 (2025) 116005

Contents lists available at ScienceDirect

Renewable and Sustainable Energy Reviews

journal homepage: www.elsevier.com/locate/rser

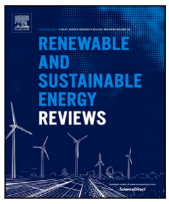

Review article

A review of alkaline electrolyzer technology modeling and applications for decision-making optimization in energy systems

Chunjun Huang [a],*, José Luis Rueda Torres [a], Yi Zong [b], Shi You [b], Xin Jin [b]

[a] Department of Electrical Sustainable Energy, Delft University of Technology, 2628 CD Delft, The Netherlands
[b] Department of Wind and Energy Systems, Technical University of Denmark, 2800 Kgs. Lyngby, Denmark

ARTICLE INFO

Keywords:
Alkaline electrolyzer
Power-to-hydrogen
Modeling review
Electrolyzer control
Electrolyzer operation and planning

ABSTRACT

Power-to-hydrogen systems, particularly the most mature alkaline electrolyzers (AELs), are increasingly deployed in modern energy systems due to their pivotal role in green hydrogen production and decarbonization. Proper modeling is vital for optimizing AEL lifecycle decisions, including design, operation, and investment. Despite numerous proposed models, a review focusing on their applications in system-level decision-making (e.g., operation and planning) remains lacking. This paper bridges this gap by reviewing over 100 peer-reviewed articles to offer an in-depth overview of AEL models employed in system-level decision-making. Followed by clarifying modeling requirements across different levels of AEL system analysis, three types of AEL models are classified in system-level decision-making: linear electricity–hydrogen (LEHM), nonlinear electricity–hydrogen (NEHM), and integrated electricity-heat-hydrogen models (IEHHM). This classification is based on representing the AEL with different levels of multi-physics detail and energy conversion assumptions. LEHM assumes a constant electricity-to-hydrogen conversion efficiency of typically about 60%–70%, while NEHM and IEHHM allow modeling of dynamic efficiency variations in the typical range of 60%–80%, where the IEHHM uniquely integrates thermal dynamics. Their modeling principles, characteristics, strengths, and limitations are systematically reviewed, followed by an in-depth overview of their applications and impacts across four applications: economic operation, grid services, heat recovery, and capacity planning. It reveals that LEHM, NEHM, and IEHHM are employed in 35%, 42%, and 23% of these applications, respectively. Finally, a discussion of current modeling limitations and future direction is provided. This paper offers valuable insights and guidance for selecting appropriate AEL models in decision-making studies and identifying pathways for advancing AEL modeling.

Contents

* Corresponding author.
E-mail address: C.J.Huang@tudelft.nl (C. Huang).

https://doi.org/10.1016/j.rser.2025.116005
Received 23 July 2024; Received in revised form 9 June 2025; Accepted 23 June 2025
Available online 15 July 2025

Nomenclature

Abbreviation

AEL	Alkaline Electrolyzer
AEM	Anion Exchange Membrane Electrolyzer
BOP	Balance of Plant
CE	Carbon Emission
DHS	District Heating System
EMPC	Economic Model Predictive Control
FCR	Frequency Containment Reserve
GA	Genetic Algorithm
HHV	Higher Heat Value
IEHHM	Integrated Electricity-Heat-Hydrogen Model
LCOE	Levelized Cost of Energy
LCOH	Levelized Cost of Hydrogen
LEHM	Linear Electricity–Hydrogen Model
LHV	Lower Heat Value
LPSP	Loss of Power Supply Probability
LP	Linear Programming
MILP	Mixed-integer Linear Programming
MINLP	Mixed Integer Nonlinear Programming
MIQCP	Mixed Integer Quadratically Constrained Programming
MISOCP	Mixed-Integer Second-Order Cone Programming
MPC	Model Predictive Control
NEHM	Nonlinear Electricity–Hydrogen Model
NPC	Net Present Cost
NPV	Net Present Value
NP	Nonlinear Programming
PEM	Proton Exchange Membrane Electrolyzer
PSO	Particle Swarm Optimization
PtH_2	Power-to-Hydrogen
PWL	Piecewise Linearization
QP	Quadratic Programming
SOC	State of Charge
SOEC	Solid Oxide Electrolyzer
UI	Voltage-Current

1. Introduction

Conventional fossil fuels, crucially supporting economic growth and technological advancements in modern society, face sustainability concerns due to depletion and environmental impacts, notably carbon dioxide emissions reaching a new high of over 36.8 gigatons [1]. The urgent need for sustainable energy solutions drives the growing integration of renewable energy sources. Global renewable energy capacity will soar to about 3700 gigawatts over the next five years, surpassing coal as the leading electricity source by 2025, and renewables reaching over 42% of global electricity generation by 2028 [2]. However, renewables integration into power systems is accompanied by multifaceted challenges, such as power imbalance caused by renewables' intermittency [3], and system instability due to inertia reduction [4]. Moreover, electrification using renewable power encounters limitations in addressing hard-to-abate sectors which are challenging to decarbonize via direct electrification [5], such as heavy transport, steel, aviation, chemicals, and shipping. Hydrogen emerges as a promising option for addressing these challenges. Hydrogen, especially the green hydrogen produced from power-to-hydrogen (PtH_2) like water electrolyzers using renewable power, represents a green energy carrier and fuel. It has been recognized as a pivotal mitigation decarbonization pathway in electricity and even hard-to-abate sectors. Moreover, hydrogen-based solutions such as PtH_2, hydrogen storage, and fuel cell technologies enable flexible energy conversion and storage pathways that help mitigate the intermittency of renewable generation. PtH_2 systems convert surplus renewable electricity into hydrogen during low-demand periods, which can then be stored for extended durations and later reconverted into electricity via fuel cells. When coordinated with hydrogen storage and fuel cell systems, electrolyzers can provide long-duration balancing and enhance grid flexibility [6]. Furthermore, electrolyzers can act as controllable loads, dynamically adjusting their power consumption in response to grid conditions and participating in frequency regulation services [7]. Globally, over 680 large-scale hydrogen projects, totaling an investment of $240 billion, reflect widespread adoption for decarbonization efforts, particularly in Europe, where hydrogen is anticipated to play a significant role across various sectors [8].

As a critical part of the hydrogen-based decarbonization pathway, the hydrogen production process with sufficient decarbonization is crucial. Water electrolysis-based PtH_2 is one of the critical hydrogen production approaches in a green manner that aligns with decarbonization objectives. It is reported that 192 power-to-X (X refers to various products such as hydrogen, ammonia, methanol, etc.) demonstration projects are being constructed across 32 countries, with Europe hosting the majority, approximately 154 projects [9]. State-of-the-art water electrolyzer systems are classified into four types: alkaline electrolyzer (AEL), proton exchange membrane electrolyzer (PEM), solid oxide electrolyzer (SOEC), and anion exchange membrane electrolyzer (AEM), each outlined with unique technical features in Table 1 [10–13]. Among these, AEL stands out as the most established and commercially viable technology, renowned for its cost-effectiveness, extended lifespan, and scalability to larger capacities. Furthermore, recent advancements of AELs prove that the enhanced AELs such as pressurized AELs also exhibit a favorable dynamic flexibility [14,15] as PEMs offer, enabling them to adapt to the fluctuation of renewables and even provide grid frequency regulation services [7]. Accordingly, it is sparking widespread deployment of AEL projects and generating significant research interest in the technology, making AEL technologies the central focus of this paper as well.

Table 1
Comprehensive comparisons of different electrolysis technologies [10–13].

Characteristic	AEL	PEM	SOEC	AEM
Temperature [°C]	65–100	70–90	600–900	50–80
Pressure [bar]	<60	<80	<1	<30
Current density [mA/cm^2]	200–500	800–2500	260–1000	300–800
Stack unit capacity [kW]	5–6000	5–2500	<10	Up to 5
Specific energy consumption [kWh/m^3]	4.2–4.8	4.4–5.0	3.7	4.8–6.9
Nominal stack efficiency [%]	63–71	60–68	96	<67
Load range [%]	20–100	0–100	−100–100	N/A
Start-up time (cold/warm) [min]	60–120/1–5	5–10/<10s	>60/<15	N/A
Ramping up/down [%/s]	10–50/10	10–90/40.6	0.1–0.3/3	N/A
Stack lifetime [kh]	55–120	60–100	8–20	N/A
CAPEX cost [€/kW]	800–1500	1400–2100	>2000	N/A
Advantages	High maturity and commercialization; low cost; long lifetime; large stack size	High flexibility; good ability to adapt renewables; high current density	High energy efficiency; less electricity consumption	Low cost; high flexibility; good ability to adapt renewables
Disadvantages	Low current density; low flexibility; long start-up time; mixing of gases	High membrane cost; short lifetime	High cost; severe environment; immature	Immature

Modeling of AEL technologies is a crucial tool for understanding their principles, optimizing system design, and enabling effective control and operation for improving their techno-economic performance. Numerous studies have been conducted to develop models for AELs at various levels of detail and dimensionality to capture the multi-physics and multiscale nature of electrolyzers. However, limited studies provide a comprehensive review of thoroughly summarizing and discussing the developed models. Only several modeling reviews of AELs [16–18] can be found. Specifically, the authors in [16] clarified models for both AELs and PEMs according to physical domains. These AEL models cover the electrical domain [19,20], electrochemical domain [21,22], and thermal domain [23–25]. Moreover, the modeling approaches are reviewed including physical law-based analytical modeling [21,22,24] and data-driven empirical modeling [23,26]. Furthermore, Ref. [17] reviews the existing mathematical modeling of AELs including thermodynamic, electrochemical, thermal, and gas purity models. Compared to [16], this review especially updates the advancement of the gas purity model considering the gas crossover phenomenon [27–31], along with presenting the modeling guideline to connect different submodels, summarizing the effects of model's parameters and operating conditions on AEL performance. Moreover, the latest modeling review of AELs is presented in [18]. It adds additional information about two-phase flow models [32–36] which characterize the interaction of gas bubbles and liquid electrolytes and its impact on the consumed electricity for producing hydrogen, compared to reviews [16,17].

Table 2 shows a comparative summary of the previous three reviews for AEL modeling. It indicates that existing reviews have contributed to comprehensively summarizing the model development of AELs covering various physical domains, aiming to characterize the complex multi-physics within AEL systems. However, a research gap still remains. That is, none of the reviews gives a clear summary and discussion of AEL model development from the perspective of system-level decision-making optimization studies involving their operation and planning within energy systems. Such studies involve distinguishing requirements of model granularity and physics representation of AELs. It is unclear how developed models have been used to represent AELs at different granularity in their decision-making optimization studies.

To address the identified research gap, this paper, by reviewing over 100 peer-reviewed articles related to system-level AEL modeling, offers a comprehensive overview of alternative AEL model development and provides a detailed summary of their utilization in optimizing decision-making for AEL systems. Overall, this work serves as a valuable guideline for both experienced modelers and beginners in selecting suitable AEL models for such decision-making optimizations. Additionally, it sheds light on the future trajectory of model advancement, particularly concerning the optimal integration of AELs into integrated energy systems. The key novel contributions of this study are as follows:

Table 2
Comparative summary among prior modeling reviews of AELs.

Modeling	Review [16]	Review [17]	Review [18]
Electrochemical models	√	√	√
Electrical models	√	×	×
Thermal models	√	√	√
Mass transfer models	×	√	√
Two-phase models	×	×	√
Models for operation and planning decision-making optimization[a]	×	×	×

[a] This term refers to a comprehensive summary of AEL models in diverse operation and planning decision-making optimization applications, which is the unique contribution of this paper.

(1) Provide a holistic analysis of hierarchical AEL research, revealing the research focus and corresponding model granularities and timeframes across different levels of AEL system analysis.

(2) Systematically sort and summarize the current state of AEL modeling in system-level decision-making optimization, categorized into three types: linear electricity–hydrogen model, nonlinear electricity–hydrogen model, integrated electricity-heat-hydrogen model.

(3) Provide a review of AEL system-level decision-making studies from the perspective of how AELs are modeled and represented in operation and planning optimization, including four specific applications: economic operation, grid service, heat recovery management, and capacity planning.

(4) Summarize in detail the utilization, features, and impact of AEL models, as well as optimization techniques development, on addressing system-level optimization.

(5) Critically discuss the advantages and disadvantages of existing models and offer insights into future directions for modeling efforts.

The rest of the paper is organized as follows: Section 2 provides a foundational understanding of AELs, including their basic principles, system structure, and a holistic overview of hierarchical analysis and modeling needs in AEL research. Section 3 offers an overview of AEL models tailored explicitly for system-level decision-making optimization studies, while Section 4 reviews examples of such studies, discussing the application of these models. Section 5 critically discusses and summarizes AEL models and their applications, while also analyzing existing deficiencies in AEL modeling and proposing future

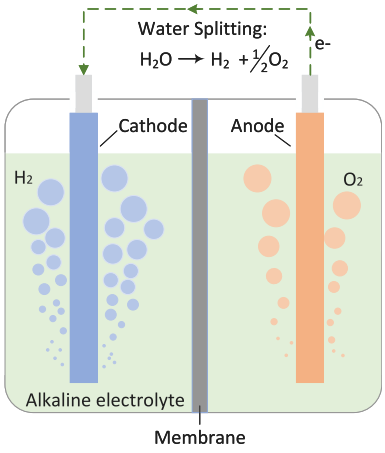

Fig. 1. Electrolyzer cell structure and electrolysis principle.

advancements. Specifically, Sections 3 to 5 constitute the core review content, offering a multi-layered assessment of AEL models, from their modeling granularity (Section 3), to their practical applications in decision-making optimization (Section 4), and finally to critical evaluations and future research pathways (Section 5). Finally, Section 6 concludes the key findings, and suggests potential directions for future research and development in AEL models.

2. Foundational understanding and modeling of alkaline electrolyzers

2.1. Basic principle and system structure

The principle behind AEL systems is to utilize electricity for the water electrolysis, resulting in the separation of hydrogen and oxygen gases. At the heart of the AEL system lies the electrolyzer cell, where the electrolysis reaction occurs. This cell comprises key components such as electrodes (including cathode and anode electrodes), a membrane, and alkaline electrolyte, as depicted in Fig. 1. Within the electrolyzer, an alkaline electrolyte solution fills the compartments divided by the membrane into cathode and anode sections. The electrolysis process, described by Eqs. (1)–(3) [23], involves the application of a direct-current (DC) to prompt electrons to flow toward the cathode, where they combine with hydrogen ions, yielding hydrogen gas. Meanwhile, hydroxide ions migrate to the anode, releasing electrons and generating oxygen gas. The electrons complete the circuit by returning to the positive pole of the power supply. Macroscopically, Fig. 2 illustrates the mass and energy flow within AEL systems, where water serves as the feedstock, leading to the main products of hydrogen gas and oxygen gas. Additionally, waste heat released during electrolysis is another valuable product, which can be recovered and utilized for heat supply. The energy required for this process is DC electricity, which can be converted from alternating-current (AC) using converters in power systems.

$$Anode: 2OH^-(aq) \rightarrow \frac{1}{2}O_2(g) + H_2O(l) + 2e^- \quad (1)$$

$$Cathode: 2H_2O(l) + 2e^- \rightarrow H_2(g) + 2H^-(aq) \quad (2)$$

$$Overall: H_2O(l) \rightarrow H_2(g) + \frac{1}{2}O_2(g) \quad (3)$$

In addition to the core component, i.e. electrolyzer cell, there are other auxiliary units within AEL systems for supporting the sustainable electrolysis process and obtaining high-purity hydrogen. Fig. 3 depicts a generalized AEL system schematic comprising the stack, balance of plant (BOP), and converter. The stack consists of multiple electrolyzer cells, where the electrolysis reaction takes place. The BOP plays a critical role in maintaining optimal conditions for electrolysis, including temperature, pressure, and electrolyte circulation, while facilitating gas product extraction and purification. Coordination among various BOP components (such as heat exchangers, pumps, gas-liquid separators, condensers, and purification systems) is essential for these functions. Converters aim to transform AC power into DC power for the stack and other BOP devices.

2.2. Hierarchical analysis and modeling needs in AEL research

Striving to advance the frontiers of AEL technology consistently requires addressing diverse levels. Drawing upon the universal framework of process control and optimization in manufacturing [37], a graphical overview of hierarchical AEL studies spanning multiple timeframes can be established, as depicted in Fig. 4. It portrays the hierarchical levels of research in AEL technology involving six levels with distinguished timeframes. From the lowest Level 1 to the highest Level 6, the studied objects extend from a single device (e.g., sensor units and control valves) within AEL systems to the whole system, along with increasing time resolutions from high-resolution (such as seconds) to lower-resolution (such as weeks or years), and reduced model granularity from fine-grained to coarse-grained. To provide a clearer structure, the AEL research hierarchy can be categorized into three primary layers: Basic Layer, Control Layer, and Optimization Layer:

(1) Basic Layer (Level 1 and Level 2): focuses on ensuring accurate data acquisition and basic equipment protection. This layer deals with real-time (e.g. no more than one second) operations like sensor validation, actuator functioning, and safety mechanisms, ensuring the immediate protection and correct functioning of hardware components. Given its focus on measurement and protection, the modeling requirements for the layer are minimal and generally straightforward. The primary concern here is the reliability and accuracy of sensor data rather than the detailed dynamics of the AEL processes. Thus, while this layer is fundamental for the real-time operation of AEL systems, it does not necessitate detailed process modeling. Its emphasis is more on robust and reliable hardware functioning rather than on extensive computational modeling.

(2) Control Layer (Level 3 and Level 4): deals with component-level control within AEL systems in timeframes from seconds up to days, ensuring their successful operation by focusing on dynamic process control within a single AEL system. This layer includes tasks related to basic control such as PID control for a single process variable (e.g., electrolyte flow rate), as well as more advanced multivariable and constraint control to handle complex interdependencies within the system (e.g., temperature, pressure, and electrolyte flow rate). This layer ensures the successful and efficient operation of AEL systems through dynamic and component-level process control. Given the needs of dealing with component-level control, the model must capture intricate details of various process dynamics, particularly the temporal variations of system operating parameters such as temperature, pressure, gas production, and supplied current/voltage. This extent of detail is crucial for designing stable and accurate controllers to regulate parameters to their desired values. Accordingly, fine-grained models with small timeframes are usually employed at this level to ensure the successful and efficient operation of AEL systems through dynamic and component-level process control.

(3) Optimization Layer (Level 5 and Level 6): addresses system-level decision-making optimization on operation and planning aspects of single and multiple AEL systems when integrated into energy systems. This layer involves activities such as economic scheduling and strategic planning to align with long-term goals. The focus here shifts to maximizing operational efficiency and economic benefits over extended periods (hours to months), covering the entire AEL system or AEL-integrated energy systems. In this layer, the models employed here usually focus on longer timeframes in which system parameters already reach their steady-state, thereby ignoring fast process

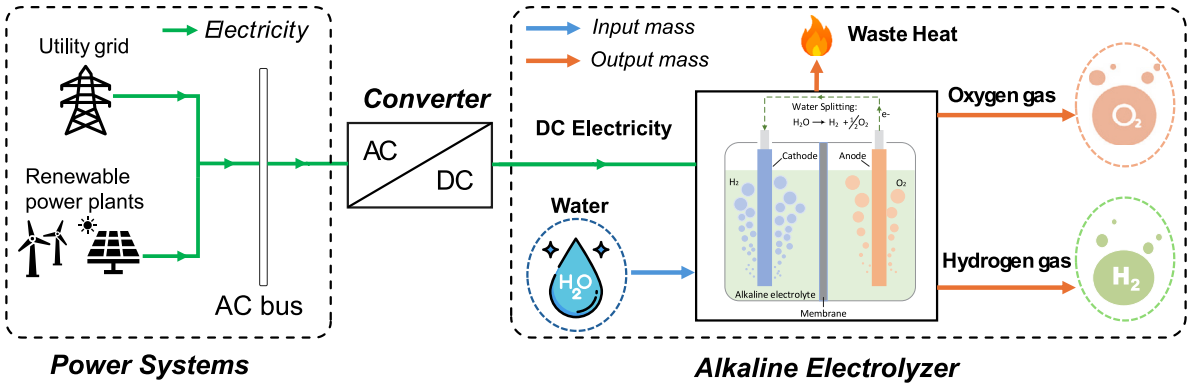

Fig. 2. Mass and energy flow within AEL systems.

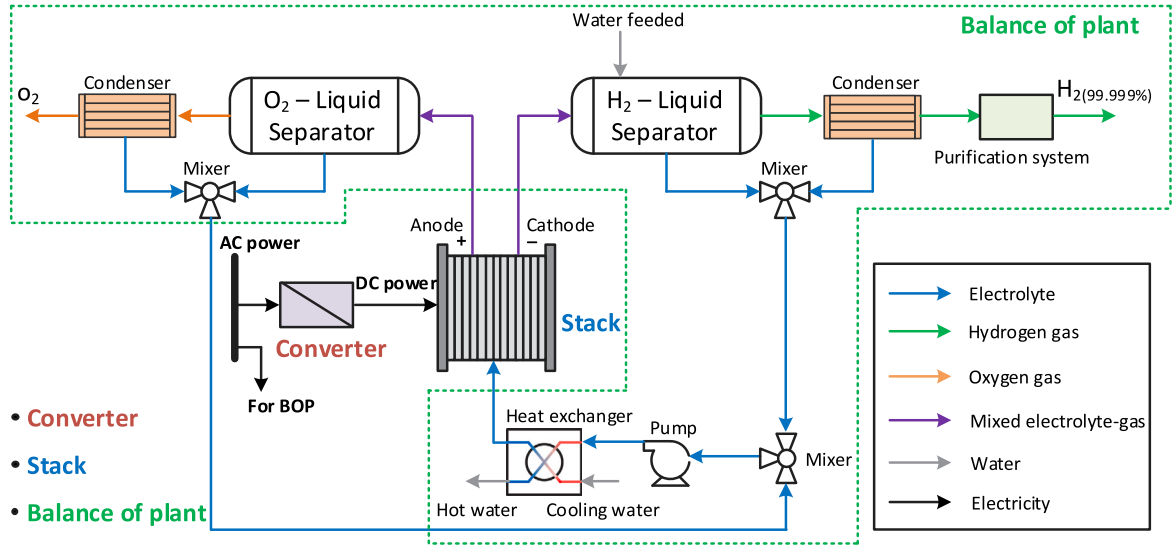

Fig. 3. Schematic of an electrolyzer system.

dynamics. To avoid a large computational burden in solving optimization models for operation and planning, using complex models representing many details of AEL is undesirable. Thus, the operation and planning of AEL systems use relatively coarse-grained models. These models usually represent high-level characteristics like the relationship between consumed electricity and obtained hydrogen production while simplifying or overlooking many details of process dynamics.

In summary, research into AEL technology includes multiple levels and layers, where model granularity and complexity exhibit significant variation. The basic layer focuses on accurate measurements and safety mechanisms, requiring minimal modeling efforts. The control layer demands highly detailed models for dynamic process control, and the optimization layer utilizes more abstracted models to facilitate long-term planning and system-level decisions. This paper will primarily focus on the modeling requirements and analysis within the optimization layer study. The reason for this focus is that system-level decision-making optimization plays a crucial role in integrating AEL systems into broader energy networks, improving overall system efficiency, and reducing operational costs. By understanding and optimizing these higher-level interactions and planning strategies, we can significantly enhance the feasibility and economic viability of implementing AEL technologies on a large scale.

3. Overview of AEL models in decision-making optimization studies

Various AEL models have been developed over the past several decades, aiming to capture complex multi-physics of AEL systems across different aspects. Fig. 5 shows the distribution of AEL modeling publications focusing on different electrolyzer model categories since 1990. The horizontal bars show the percentage of studies that investigate the corresponding model. These models can be divided into five categories for characterizing different phenomena, including electrochemical [16,17,21–23,26,29,31,38–53], gas crossover [28–31,54–56], thermal [21,23,24,41,57,58], two-phase flow models [32–36,59–63], and thermodynamic models [21,23]. Notably, many efforts are put into electrochemical models in order to capture the key characteristics of AELs (including polarization curve, hydrogen production rate, and system efficiency) and their dependency on operation parameters.

Those established models are instrumental in precisely predicting the multi-physics phenomena (electricity-heat-hydrogen interactions) and interdependent process dynamics (such as hydrogen production rate, temperature change, and gas transfer) within AEL systems. Consequently, they play a crucial role in guiding system design optimization and facilitating the development of advanced control strategies. However, given the granularity requirements across different system-level

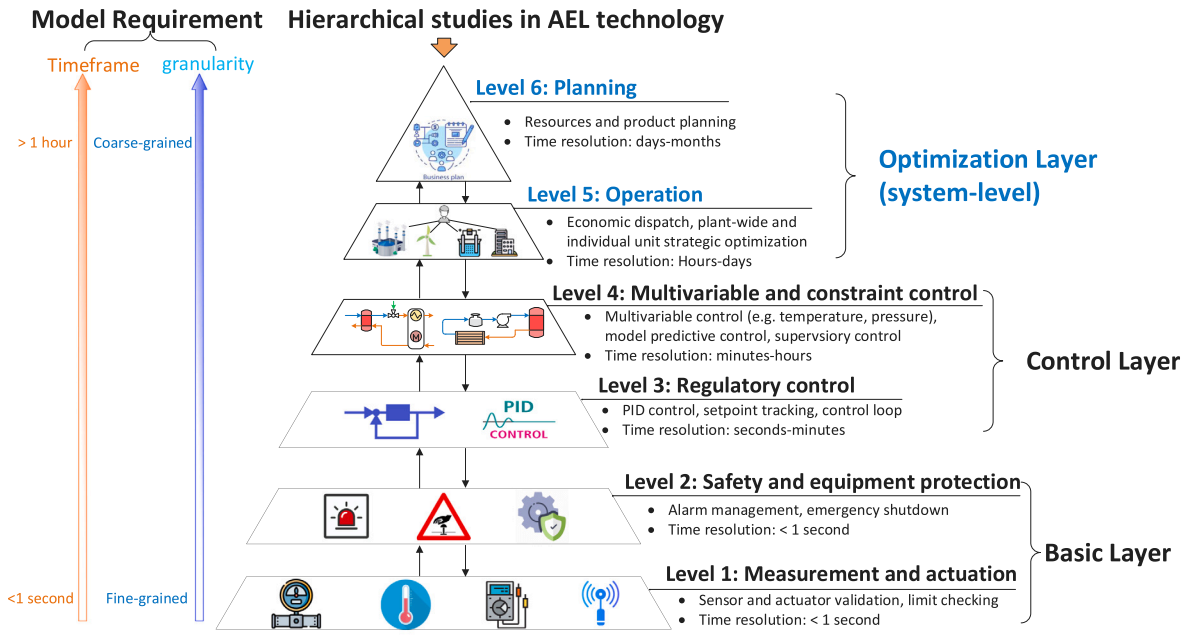

Fig. 4. Hierarchical overview of AEL research (inspired by [37]).

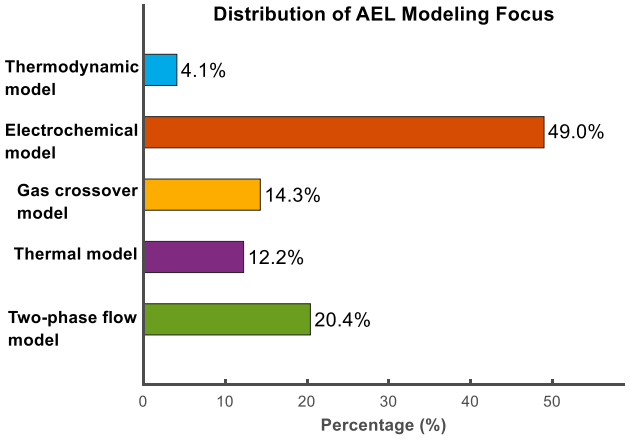

Fig. 5. Distribution of AEL modeling studies since 1990 that focusing on thermodynamic, electrochemical, gas crossover, thermal, and two-phase flow modeling, respectively [16–18].

decision-making optimization, it remains unclear how these models are selected, combined, and simplified in various AEL optimization studies to approximately represent the AEL system. Mapping AEL models to their system-level decision-making optimization studies needs further development.

To address this gap, this review specifically focuses on AEL models that are applied in system-level decision-making optimization including tasks such as economic dispatch and capacity planning. These applications typically correspond to Levels 5–6 of the framework shown in Fig. 4, which involve daily to hourly time resolutions and prioritize computational tractability. Within this scope, AEL models are classified into three representative categories according to their level of physical accuracy in representing energy conversion processes:

- Linear electricity–hydrogen model (LEHM)
- Nonlinear electricity–hydrogen model (NEHM)
- Integrated electricity-heat-hydrogen model (IEHHM)

These three categories reflect the dominant modeling approaches used in system-level optimization studies, and they are selected based on how effectively they balance physical accuracy and computational complexity in practical optimization formulations. Notably, other modeling approaches, typically dynamic, stochastic, hybrid, and economic-coupled models, are also used for system-level optimization of AEL-integrated energy systems. However, these are not treated as standalone AEL model types in our classification for the following reasons:

(1) Dynamic models are primarily developed for control applications and transient simulations at millisecond-to-second time scales. Their high temporal resolution and computational demands make them unsuitable for long time-horizon system optimization;

(2) Stochastic models typically relate to uncertainty in system-level parameters (e.g., wind generation, market prices), and not to the inherent structure of AEL models. They apply to the overall optimization formulation, not to the electrolyzer model itself;

(3) Hybrid models, such as combining machine learning with physical models, are often used to enhance prediction accuracy within NEHM or IEHHM. However, they do not form a separate structural model class at the device level;

(4) Economic-coupled models refer to the energy system's optimization model integrating economic objectives (e.g., revenue maximization) and do not affect the physical formulation of AEL devices.

Therefore, these modeling approaches are not treated as separate AEL model types in our classification. Instead, this review focuses on three representative models (i.e. LEHM, NEHM, and IEHHM) which serve as the primary device-level formulations tailored for system-level decision-making optimization. Thus, the majority of this section (Sections 3.1–3.4) will delve into the specific principles, characteristics, formulations, and comparative insights of these three model types. In addition, the relevance between these three AEL models and optimization models of AEL-integrated energy systems, such as the earlier-mentioned stochastic or economic-coupled model, will be clarified in Section 3.5.

3.1. Linear electricity–hydrogen model

The linear electricity–hydrogen model is the simplest one, and it assumes that AEL is seen as an energy converter for which electrical power is supplied to produce an amount of hydrogen gas. This model is essentially a black-box model that only offers a high-level description

of the energy conversion relationship of AEL devices rather than precise characterizations of physical phenomena inside the AEL cell and system. The relationship between consumed electrical power P_{AEL} and hydrogen production rate $\dot{m}_{\mathrm{H}_2}$ is the core of this model, which can be generically expressed by Eq. (4) [64–70].

$$\dot{m}_{\mathrm{H}_2} = K_{ecr} P_{AEL} = \frac{\eta P_{AEL}}{Q_{\mathrm{H}_2}} \tag{4}$$

where K_{ecr} denotes the conversion rate from electrical power to hydrogen production; η is the AEL's system efficiency; Q_{H_2} is the heat value of hydrogen; either the higher heat value (HHV) [71] or lower heat value (LHV) [6] has been used in existing studies.

The linear electricity–hydrogen model assumes a constant conversion rate K_{cr} or system efficiency η that are not affected by consumed power and other operation parameters of AEL such as temperature and pressure. Thus, the technical aspects of AELs in this model, are considered by enforcing limits on consumed electrical power within a certain range and obtaining corresponding hydrogen production rate based on a given conversion rate or system efficiency. The process of operational mode transition of AELs can be integrated with this model. Two operational modes including On (production mode) and Off are considered by introducing a binary variable [64,65,67]. Furthermore, introducing more binary variables can enable more modes including On, Standby, off, as well as their switching process [69,72].

Additionally, a linear electricity–hydrogen model can also be coupled with the state of charge (SOC) description of hydrogen energy storage systems, as formulated by Eq. (5). Such a coupled model is usually employed when conducting co-dispatch and co-planning between AELs and other hydrogen facilities in microgrids or power systems [65,67,69,73]. An example of this coupling is formulated by Eq. (6) which characterizes the constraints among electrolyzers, hydrogen tanks, and fuel cells, while only considering the On/Off state of AELs.

$$SOC_{t+1} = SOC_t + \dot{m}_{\mathrm{H}_2} T_s - f(\mathrm{H}_2) \tag{5}$$

$$SOC_{t+1} = SOC_t + \delta_{ely} \frac{\eta P_{AEL}}{Q_{\mathrm{H}_2}} T_s - \delta_{fc} \frac{P_{fc}}{\eta_{fc} Q_{\mathrm{H}_2}} T_s \tag{6}$$

where T_s is the time-resolution in operation and planning studies; $f(\mathrm{H}_2)$ represents the hydrogen demand of hydrogen consumers over T_s, such as fuel cells and ammonia production industry; η_{fc} denotes the efficiency of the fuel cell. Binary variables $\delta_{ely}, \delta_{fc}$ identify the On/Off state of the AEL and fuel cell.

Due to only focusing on system-level description of energy conversion relation, the linear electricity–hydrogen model is mostly utilized for decision-making optimization of AEL operation and planning within energy systems. Moreover, owing to the assumption of fixed system efficiency, this model exhibits a linear relation between consumed power and hydrogen production, This fact drives that optimization models of decision-making problems can be directly formulated into linear programming (LP) [64] or mixed integer linear programming (MILP) [65–67,70] which can be easily solved via commercial solvers like Gurobi [74].

3.2. Nonlinear electricity–hydrogen model

The assumption of fixed system efficiency in the linear electricity–hydrogen model overlooks a real characteristic of AELs, which is that efficiency varies with operational parameters such as consumed power, temperature, and pressure. This assumption potentially inaccurately estimates hydrogen production outputs and states of AEL systems, causing the infeasibility of control actions and decision-making solutions. To address this issue, the nonlinear electricity–hydrogen model is introduced by considering the efficiency variations.

3.2.1. Efficiency variation

According to Eq. (4), the system efficiency is described as the ratio of consumed electrical energy to produced hydrogen energy. It is formulated by Eq. (7) where the Q_{H_2} is set as HHV because the HHV of hydrogen is often chosen for the efficiency calculation in low-temperature electrolyzers [6]. Based on the Faraday law, the hydrogen production rate $\dot{m}_{\mathrm{H}_2}$ is directly proportional to input current I, as expressed by Eq. (8). The coefficient η_F is the Faraday efficiency, which measures the ratio of actual hydrogen production to its theoretical value [6]. Substituting Eq. (8) into Eq. (7), the system efficiency can be reformulated by Eq. (9). Particularly, the second term of Eq. (9) corresponds to another efficiency metric, voltage efficiency, defined in Eq. (10) as the ratio between the thermoneutral voltage (U_{tn}) and the actual cell voltage (U_{cell}). This metric reflects the magnitude of overpotential within electrolyzer cells. The presented voltage efficiency formulation is derived in Appendix. Thus, the system efficiency is equal to the product of the Faraday efficiency and voltage efficiency, as formulated by Eq. (11).Unless otherwise specified, the term "efficiency" for AELs in the manuscript refers to the system efficiency.

$$\eta = \frac{\dot{m}_{\mathrm{H}_2} HHV}{P_{AEL}} = \frac{\dot{m}_{\mathrm{H}_2} HHV}{N_{cell} U_{cell} I} \tag{7}$$

$$\dot{m}_{\mathrm{H}_2} = N_{cell} \eta_F \frac{I}{zF} M_{\mathrm{H}_2} \times 3600 \tag{8}$$

$$\eta = \eta_F \cdot \frac{3600 M_{\mathrm{H}_2} \cdot HHV}{zF U_{cell}} \tag{9}$$

$$\eta_v = \frac{U_{tn}}{U_{cell}} \tag{10}$$

$$\eta = \eta_F \cdot \eta_v = \eta_F \cdot \frac{U_{tn}}{U_{cell}} \tag{11}$$

where N_{cell} is the number of cells within one stack; z is the number of transferred electrons per electrolysis reaction; F is the Faraday constant; M_{H_2} is the molar mass of hydrogen; U_{tn} is the thermoneutral voltage; its calculation is given in Appendix.

Regarding the Faraday efficiency, two different empirical models have been developed in existing studies to calculate it, as shown in Eq. (12) [23] and Eq. (13) [31]. It indicates the Faraday efficiency depends on the input current I to the AEL. Additionally, the cell voltage U_{cell} is obtained based on the polarization characteristics also known as the voltage-current (UI) curve which characterizes the relationship between cell voltage and input current. This curve can be mathematically modeled as Eq. (14). It indicates that the cell voltage consists of a few terms including reversible voltage U_{rev}, activation overvoltage U_{act}, ohmic overvoltage U_{ohm}, and diffusion overvoltage U_{diff}.

$$\eta_F = \frac{(I/A)^2}{f_1 + (I/A)^2} f_2 \tag{12}$$

$$\eta_F = B_1 + B_2 \cdot e^{\frac{B_3 + B_4 T + B_5 T^2}{I}} \tag{13}$$

$$U_{cell} = U_{rev} + U_{act} + U_{ohm} + U_{diff} \tag{14}$$

where f_1, f_2 and $B_1 \sim B_5$ are fitted parameters for empirical models. These coefficients are obtained through empirical regression and do not carry explicit physical meaning. The reversible voltage is the theoretical minimum cell voltage required for the electrolysis reaction. The later three terms in Eq. (14) represented the overpotentials that arise from the kinetics of the electronic charge transfer, mass transfer and ohmic losses in electrolytes.

A few existing reviews have provided comprehensive summaries of various electrochemical modeling approaches proposed in prior literature to characterize cell voltage, including both physical law derived mechanism models and data-driven empirical models [16–18]. Detailed explanations of all those models are thus not repeated in this paper. An example of such models is presented to illustrate how the cell voltage can be calculated, as expressed in Eq. (15), which is a widely utilized empirical model proposed in [23]. To obtain the reversible voltage

in Eq. (15), several models have been proposed [16–18]. A specific model [43,46] can be expressed by Eqs. (16)–(22).

$$U_{cell} = U_{rev} + \frac{(r_1 + r_2 \cdot T)}{A} I + s \cdot \log\left(\left(t_1 + \frac{t_2}{T} + \frac{t_3}{T^2}\right) \cdot \frac{I}{A} + 1\right) \tag{15}$$

$$U_{rev} = U^0_{rev} + \frac{R(T+273.15)}{zF} \ln\left(\frac{(P - P_{v,KOH})^{1.5}}{\alpha_{H_2O}}\right) \tag{16}$$

$$U^0_{rev} = 1.5184 - 1.5421 \times 10^{-3}(T+273.15) + 9.523 \times 10^{-5}(T+273.15) \cdot \ln(T+273.15) + 9.84 \times 10^{-8}(T+273.15)^2 \tag{17}$$

$$P_{v,KOH} = \exp\left(2.302a + b \ln P_{v,H2O}\right) \tag{18}$$

$$a = -0.0151\ m - 1.6788 \times 10^{-3} m^2 + 2.2588 \times 10^{-5} m^3 \tag{19}$$

$$b = 1 - 1.2062 \times 10^{-3} m + 5.6024 \times 10^{-4} m^2 - 7.8228 \times 10^{-6} m^3 \tag{20}$$

$$P_{v,H2O} = \exp\left(81.6179 - \frac{7699.68}{T+273.15} - 10.9 \cdot \ln(T+273.15) + 9.5891 \times 10^{-3}(T+273.15)\right) \tag{21}$$

$$\alpha_{H_2O} = \exp\left(-0.05192\ m + 0.003302 m^2 + \frac{3.177m - 2.131m^2}{T+273.15}\right) \tag{22}$$

where $r_1, r_2, s, t_1, t_2, t_3$ are fitted coefficients. These coefficients are derived through data-driven fitting techniques to mathematically capture the polarization characteristics, without implying physical interpretability. T and P are the operating temperature and pressure of the electrolyzer stack; R is the gas constant; m is the molal concentration of the alkaline solution.

The combination of Eqs. (7)–(22) forms the nonlinear electricity–hydrogen model, which can be generally expressed by Eq. (23). Notably, substituting Eqs. (12)–(22) into Eq. (11) reveals that η is influenced by the input current. Consequently, η varies with the consumed power of AELs. This dependence is captured by the nonlinear relationship derived in Eq. (23) and visualized in Fig. 6. The figure illustrates that, at a fixed temperature of 80°Celsius, both the hydrogen production rate and system efficiency change nonlinearly with power input, instead of a linear relation (i.e. the black line) captured by LEHM. Thus, this figure reveals the limitations of using LEHM for accurately estimating the hydrogen production and system efficiency.

$$\eta = f(P_{AEL}), \quad \dot{m}_{H_2} = g(P_{AEL}) \tag{23}$$

where $f(\cdot)$ and $g(\cdot)$ are nonlinear functions, characterized by Eqs. (7)–(22).

3.2.2. Approximation for nonlinear efficiency

Due to the inherent nonlinearity of the AEL model as depicted in Eq. (23), the resulting decision-making optimization models are typically non-convex and non-linear, posing substantial computational challenges. To mitigate these issues, researchers have investigated approximation methods to fit the nonlinear functions $f(\cdot)$ and $g(\cdot)$ with a low-order representation in good accuracy. The common method is to adopt a linearized and quadratic fitted form for Eq. (23).

A linear regression-based simplification of the nonlinearity in (23) has been adopted to derive the linear model shown in Eq. (24) [75,76]. Similarly, a first-order form, as expressed in Eq. (25), has also been utilized to correlate the consumed power with hydrogen production rate [77,78]. In contrast, direct linearization of Eq. (23) has been proposed to develop both linear and second-order approximations, formulated in Eqs. (26) and (27) [15]. These formulations have demonstrated that linear models are more suitable for large-scale problems with strict computational constraints, whereas the second-order models

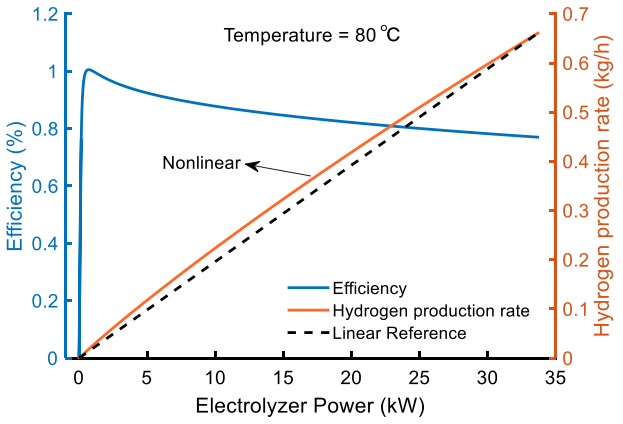

Fig. 6. Nonlinear variation of hydrogen production rate and system efficiency with consumed power at 80°Celsius. The orange line shows the hydrogen production rate, and the blue line shows system efficiency, both derived from the NEHM formulation Eq. (23). The black dashed line represents a constant-efficiency (captured by LEHM) baseline for comparison. .

provide improved accuracy for detailed estimation of hydrogen production in smaller-scale applications. The second-order formulation in Eq. (27) has also been adopted and calibrated using empirical hydrogen production data under various loading conditions, such as nominal, half, and quarter-rated power levels [79]. In addition, piecewise linear (PWL) approximation methods have been employed to improve the approximation accuracy while maintaining compatibility with common mathematical solvers (e.g. MILP). These methods approximate the nonlinear relationships between hydrogen production and consumed power (i.e. $\dot{m}_{H_2} = f(P_{AEL})$) or between consumed power and current (i.e. $P_{AEL} = h(I)$), using multiple linear segments, as described in Eqs. (28) and (29) [80–84]. In addition to linear and PWL approximations, a second-order polynomial model has been applied to approximate the power-current relationship $P_{AEL} = h(I)$, as shown in Eq. (30) [5]. Other linearization strategies, including polynomial fitting and segmented PWL, have also been introduced but without providing explicit mathematical formulations [85,86].

These approximation techniques enable the reformulation of nonlinear AEL constraints into tractable optimization models. For example, MILP formulations have been constructed by applying linear approximations [15,75,76,86], while QP models are enabled through quadratic fitting [79]. The simplified AEL constraints also facilitate the application of evolutionary algorithms in multi-objective planning studies. In particular, genetic algorithms (GA) [77,78] and particle swarm optimization (PSO) [85,87] have been successfully employed for coordinated sizing of AELs and other renewable energy technologies.

$$P_{AEL} = k \cdot \dot{m}_{H_2} \tag{24}$$

$$P_{AEL} = a_1 \cdot \dot{m}^N_{H_2} + a_2 \cdot \dot{m}_{H_2} \tag{25}$$

$$\dot{m}_{H_2} = b_1 P_{AEL} + b_2 \tag{26}$$

$$\dot{m}_{H_2} = c_1 P^2_{AEL} + c_2 P_{AEL} + c_3 \tag{27}$$

$$\dot{m}_{H_2} = \sum_{s \in S} \omega_s \dot{m}^o_{H_2}, \ P_{AEL} = \sum_{s \in S} \omega_s P^o_{AEL} \tag{28}$$

$$P_{AEL} = \sum_{s \in S} \omega_s P^o_{AEL}, \ I = \sum_{s \in S} \omega_s I^o \tag{29}$$

$$P_{AEL} = d_1 I^2 + d_2 I \tag{30}$$

where a_i, b_i, c_i, d_i are the constant coefficients obtained in various approximation methods, without possessing direct physical meaning; $\dot{m}^N_{H_2}$ is the nominal hydrogen mass flow; In piecewise linear approximation methods, the superscript o denotes the variable value at the chosen breakpoints; s is the index of each segment and S is the set

of segments; ω_s denotes the weight for linear segment s, which is a continuous variable subject to a set of linear constraints.

3.3. Integrated electricity-heat-hydrogen model

Operating temperature T, as evidenced by Eq. (15) and Appendix, significantly affects both cell voltage and thermoneutral voltage, leading to an influence on system efficiency (η) according to Eq. (11). However, the two prior electricity–hydrogen models neglect AEL temperature dynamics and their impact on the electricity–hydrogen relationship. Furthermore, AEL operation generates waste heat due to the presence of overpotentials. This waste heat via heat recovery can be utilized as a heat source for various applications, such as space heating or district heating systems. This enables the possibility of transforming the waste heat into a co-product alongside hydrogen for AELs. In this context, recognizing the significance of capturing temperature dynamics and the value of waste heat, the representation of AELs can be extended from an electricity–hydrogen model to a more comprehensive electricity-to-heat-hydrogen model.

3.3.1. Thermal model of AELs

To capture the temperature changes within AEL systems, thermal dynamics need to be characterized in the electricity-to-heat-hydrogen model. To address this issue, diverse thermal models have been developed which can be categorized into three types.

Type I: A lumped thermal model (named by type I in this paper) is firstly proposed, which is widely utilized [23], as expressed by Eq. (31). This model conceptualizes the electrolyzer stack as an equivalent thermal system with lumped capacitance. It characterizes the thermal behavior within the AEL as primarily governed by three factors: (i) heat generation ($\dot{Q}_{pro}$) during the electrolysis reaction, influenced by the input current or power; (ii) heat loss ($\dot{Q}_{loss}$) to the surroundings occurs due to the temperature difference between the AEL and the ambient environment; (iii) heat extracted ($\dot{Q}_{cool}$) by the circling electrolyte which will be cooled through a heat exchanger via flowing cooling water inside. $\dot{Q}_{pro}$ and $\dot{Q}_{loss}$ can be calculated by Eqs. (32)–(33). $\dot{Q}_{cool}$ would be controlled to maintain the AEL temperature at the desired level, which is determined by different ways in existing studies.

In Type I model, the heat exchanger model is integrated to calculate the $\dot{Q}_{cool}$, which can be expressed by Eqs. (34)–(35). Note that the $LMTD_{he}$ expression is based on an assumption that the inlet and outlet electrolyte temperature inside the heat exchanger are same. This implies that the Ulleberg's model assumes a homogeneous temperature distribution within the AEL system and only predicts the average temperature T of the system.

$$C_{ely}\frac{dT}{dt} = \dot{Q}_{pro} - \dot{Q}_{loss} - \dot{Q}_{cool} \tag{31}$$

$$\dot{Q}_{pro} = N_{cell}U_{cell}I(1-\eta_{tot}) = P_{AEL}(1-\eta) \tag{32}$$

$$\dot{Q}_{loss} = \frac{T-T_a}{R_{heat}} \tag{33}$$

$$\dot{Q}_{cool} = \dot{m}_{cool}c_{cw}(T_{cw,i}-T_{cw,o}) = U_{he}A_{he}LMTD_{he} \tag{34}$$

$$LMTD_{he} = \frac{(T-T_{cw,i})-(T-T_{cw,o})}{\ln\frac{T-T_{cw,i}}{T-T_{cw,o}}} \tag{35}$$

where C_{ely} refers to the lumped thermal capacitance of the AEL stack.

Based on the above first-order differential equations Eqs. (31)–(35), the nonlinear solution of the temperature can be derived as Eqs. (36)–(38). Particularly, it is observed that the temperature T can be controlled by adjusting the mass flow rate $\dot{m}_{cool}$ of the cooling water. Hence, a PI controller is developed for adjusting $\dot{m}_{cool}$ in order to enable T to precisely track its reference [88]. This controller can be expressed by Eq. (39).

$$T(t) = \left(T_{ini} - \frac{b}{a}\right)\exp(-at) + \frac{b}{a} \tag{36}$$

$$a = \frac{1}{\tau_t} + \frac{\dot{m}_{cool}c_{cw}}{C_{ely}}\left[1-\exp\left(-\frac{U_{he}A_{he}}{\dot{m}_{cool}c_{cw}}\right)\right] \tag{37}$$

$$b = \frac{N_{cell}U_{cell}I(1-\eta)}{C_{ely}} + \frac{T_a}{\tau_t} + \frac{\dot{m}_{cool}c_{cw}T_{cw,i}}{C_{ely}}\left[1-\exp\left(-\frac{U_{he}A_{he}}{\dot{m}_{cool}c_{cw}}\right)\right] \tag{38}$$

$$\dot{m}_{cool} = \rho_{cw}k_n\frac{1}{1+t_d s}\cdot(T-T_{ref})\left(k_p + \frac{k_i}{s}\right) \tag{39}$$

where s is the Laplace operator.

Type II: The calculation of $\dot{Q}_{cool}$ in Type I model is further modified by addressing the assumption in the $LMTD_{he}$ expression [79]. The calculation method accounts for the difference between the inlet and outlet electrolyte temperature inside the heat exchanger, and considers the outlet electrolyte temperature equals the stack temperature. Accordingly, a new model (named by type II) is proposed, as formulated by Eqs. (40)–(41) combined with Eqs. (31)–(33).

$$\dot{Q}_{cool} = \dot{m}_{liq}c_{liq}(T_{liq,i}-T) = \dot{m}_{cool}c_{cw}(T_{cw,o}-T_{cw,i}) \tag{40}$$

$$\dot{Q}_{cool} = U_{he}A_{he}\frac{(T-T_{cw,i})-(T_{liq,i}-T_{cw,o})}{\ln\frac{T-T_{cw,i}}{T_{liq,i}-T_{cw,o}}} \tag{41}$$

where $T_{liq,i}$ is the inlet electrolyte temperature inside the heat exchanger;

Type III: Furthermore, the above Type I model is also upgraded by augmenting the thermal balance relationship Eq. (31) with the introduction of an additional term $\dot{Q}_{exch}$ [17,21,24]. This term accounts for the total heat exchange occurring with the exiting hydrogen and oxygen streams, including both their sensible and latent heat components. Additionally, it incorporates the sensible heat necessary to elevate the temperature of deionized water from ambient to the operating temperature of the stack. This enhanced consideration offers a more precise representation of the heat transfer processes within the AEL. The corresponding model (named by type III) can be expressed by [17,21,24]:

$$C_{ely}\frac{dT}{dt} = \dot{Q}_{pro} - \dot{Q}_{loss} - \dot{Q}_{cool} - \dot{Q}_{exch} \tag{42}$$

$$\dot{Q}_{loss} = A_{stack}\cdot h\cdot(T_{stack}-T_a) = \frac{T-T_a}{R_{heat}} \tag{43}$$

$$h = 1.32\cdot\left(\frac{\Delta T}{\phi}\right)^{0.25} \quad \text{or} \quad h = h_0 + k\cdot I \tag{44}$$

$$\dot{Q}_{exch} = \dot{m}_{H_2}\cdot C_p^{H_2}(T-T_a) + \cdot\dot{m}_{O_2}C_p^{O_2}(T-T_a) + \dot{m}_{H_2O}\cdot C_p^{H_2O}(T-T_{in}^{w}) + \dot{m}_{vapor}\lambda_{H_2O} \tag{45}$$

$$\dot{m}_{H_2O} = \dot{m}_{H_2} + \dot{m}_{O_2} + \dot{m}_{vapor} \tag{46}$$

$$\dot{m}_{H_2} = 0.125\dot{m}_{O_2} \tag{47}$$

where $\dot{Q}_{pro}$ and $\dot{Q}_{cool}$ can be calculated by Eq. (32) and Eqs. (34)–(35), respectively;

Further developments have extended beyond the first-order thermal models that characterize only the temperature dynamics of the AEL stack. Several studies have incorporated the thermal behavior of the gas-liquid separator to provide a more complete representation of the full AEL system. A second-order model that considers the thermal capacitance of both the stack and the gas-liquid separator has been proposed to capture this expanded thermal behavior [58]. A third-order formulation has also been introduced, in which the thermal balances of the stack, the hot side, and the cold side of the heat exchanger are modeled independently [57]. This improves the granularity of thermal representation. Additionally, a third-order time-delay model has been developed to predict both pre-stack and post-stack temperatures, while accounting for inherent thermal delays arising from the stack and the downstream cooling coil [25]. These higher-order models improve the accuracy of thermal characterization across the entire AEL system and are particularly useful in thermal control analysis. However, their

increased complexity and large parameter requirements hinder their practical application in decision-making optimization contexts. Therefore, detailed formulations of these models are not included in this review.

3.3.2. Model simplification

The integrated electricity-heat-hydrogen model exhibits strong nonlinearity due to both the nonlinear electricity–hydrogen relation $g(\cdot)$ and the nonlinear temperature response. As demonstrated in Eqs. (36)–(39), the Type I thermal model's temperature response is nonlinear, primarily due to the nonlinear terms in $\dot{Q}_{cool}$. This nonlinearity is also observed in the other two thermal models, as they similarly incorporate a nonlinear expression of $\dot{Q}_{cool}$. Consequently, integrating the electricity-heat-hydrogen model into a decision-making framework results in nonlinear optimization models, significantly increasing the computational burden for solving them. To mitigate this issue, existing studies have simplified the consideration of $\dot{Q}_{cool}$ in Type I model by neglecting the heat exchanger modeling and treating $\dot{Q}_{cool}$ as an independent decision variable [88–94] . The behind idea is to assume that the cooling power can be freely controlled without limitations imposed by heat recovery technical constraints (e.g., the interdependence between $\dot{Q}_{cool}$ and T. Additionally, this model assumes constant heat generation and transfer rates within a given time interval Δt.

Based on the aforementioned assumptions, the first-order thermal model Eq. (31) can be simplified and reformulated as Eq. (48). Combining this thermal model with the nonlinear electricity–hydrogen model Eqs. (7)–(22) establishes the integrated electricity-heat-hydrogen model, generally formulated by Eqs. (48)–(49) [88–94]. In this model, P_{AEL} and $\dot{Q}_{cool}$ serve as decision variables, while temperature T is considered a state variable. This model can be also updated by adding new terms representing additional thermal processes, such as the $\dot{Q}_{exch}$ in Type III thermal model Eq. (42), and an auxiliary heating $\dot{Q}_{heat}$ as presented in [95]. Notably, $\dot{Q}_{cool}$ representing the waste heat removed by heat exchangers, can be potentially recovered and to supply heat demands and create additional revenue by heat sales [96]. Therefore, this model captures the power-to-hydrogen-and-heat characteristics of AEL systems, enabling the calculation of both hydrogen production and recovered heat based on a given electrical power input. By incorporating heat management in decision-making optimization, the model can expand the potential for increasing AEL benefits compared to the electricity–hydrogen model.

$$T_{t+1} = T_t + \frac{\Delta t}{C_{ely}} \left(\dot{Q}_{pro} - \dot{Q}_{loss} - \dot{Q}_{cool} \right) \tag{48}$$

$$\dot{m}_{\mathrm{H_2}} = g(P_{AEL}, T(P_{AEL})) \tag{49}$$

where $\dot{Q}_{pro}$ and $\dot{Q}_{loss}$ are characterized by Eqs. (32)–(33), respectively; $\dot{Q}_{cool}$ serves as an independent decision variable in decision-making optimization rather than being characterized by Eqs. (34)–(35); and Δt represents the time interval for decision-making optimization models. The nonlinear function $g(\cdot)$ is defined by Eqs. (7)–(22).

However, the aforementioned integrated electricity-heat-hydrogen model exhibits strong nonlinearity due to two factors: (i) the nonlinear expression $P_{AEL} \cdot \eta$ within $\dot{Q}_{pro}$, as shown in Eq. (32), where a nonlinear relationship $f(\cdot)$ exists between P_{AEL} and η as shown in Eq. (23); and (ii) the nonlinear function $g(\cdot)$. To mitigate the computational challenges arising from these nonlinearities in decision-making optimization, several studies have proposed linearization techniques.

3.4. Comparative summary of AEL models

This section presents a comparative analysis of the three AEL models discussed, focusing on their system representation, formulation, efficiency characteristics, thermal dynamics considerations, model nature, applicable optimization techniques, and their respective advantages and disadvantages. Table 3 summarizes these key aspects for a comprehensive comparison.

- **LEHM:** This model adopts a simplified, black-box approach, representing only the relationship between input electrical power and hydrogen production rate (EtH relationship) through a constant system efficiency or conversion rate. Its low complexity and linear nature make it suitable for formulating decision-making optimization problems for AEL systems using LP or MILP techniques. These techniques are computationally efficient and ideal for large-scale system analysis. However, the model's simplicity comes at the cost of accuracy. By neglecting the dynamic variations of system efficiency and the influence of parameters like input power and temperature, it may not accurately capture the real-world behavior of AEL systems.
- **NEHM:** This model enhances accuracy by incorporating a physics-based approach that accounts for variable system efficiency by analyzing the polarization characteristics of AELs. This allows for a more realistic representation of the EtH relationship, capturing the impact of operational parameters on system performance. However, the inherent nonlinearities introduce greater complexity, requiring more advanced optimization techniques such as nonlinear programming for AEL decision-making optimization. While direct application of nonlinear solvers may be computationally expensive, linearization approximation techniques are usually employed to find near-optimal solutions with a manageable computational burden. However, this inevitably leads to some loss of accuracy due to the approximation.
- **IEHHM:** This model offers the most comprehensive analysis by considering the coupled relationship between electricity, heat, and hydrogen production (EtHH relationship). It incorporates the variable system efficiency, polarization curve characteristics, and, uniquely, detailed thermal dynamics modeling. This inclusion of thermal dynamics is a unique feature that enables the model to be used for investigating AEL thermal management strategies and their impacts, such as designing efficient cooling control methods for both efficiency and temperature safety. Additionally, it allows for assessing the potential for waste heat recovery by quantifying the amount of waste heat generated, thereby contributing to improved overall system sustainability and economic feasibility. Moreover, the integrated approach enables simultaneous optimization of the AEL's dual products, including hydrogen production and waste heat recovery, based on a given input electrical power, maximizing overall energy efficiency and economic benefits, especially when AELs are integrated with other thermal processes or energy systems like district heating. However, this EtHH coupling and inherent nonlinearities within this model bring the highest complexity compared to other models, necessitating sophisticated optimization techniques like nonlinear programming. Linearization approximation is usually needed for computational feasibility, leading to some loss of accuracy. While computationally demanding, this model offers the highest level of precision and a more comprehensive understanding of the AEL system behavior.

The above comparison clarifies the differences in modeling accuracy, mathematical complexity, and physical coverage among LEHM, NEHM, and IEHHM, thus offering a practical guide for model selection and development. For practitioners and researchers, this comparative structure provides a clear basis for aligning model complexity with specific application demands, including long-term planning, short-term dispatch, and thermal-energy integration. In practice, the selection of the most suitable AEL model generally follows the principles below:

(i) LEHM is recommended for large-scale system planning and operational scheduling tasks, where computational simplicity and solver tractability are prioritized;

(ii) NEHM is appropriate for detailed performance analysis and optimization of AELs, providing a balance between accuracy and tractability, especially when variable efficiency needs to be captured;

Table 3
Comparative analysis of AEL models for decision-making optimization.

Characteristics	LEHM	NEHM	IEHHM
System Description	Black-box representation: EtH relationship[a]	Physics-based approach: EtH relationship with variable efficiency and polarization curve	Physics-based approach: EtHH relationship[b] with variable efficiency, polarization curve, and thermal dynamics
Formulation	Eq. (4)	Eq. (23)	Eqs.(32)–(33), (48)–(49)
System Efficiency	Constant	Dependent[c]	Dependent
Thermal Dynamics	Not considered	Not considered, temperature (T) is an input parameter	Included, with T as a state variable and waste heat recovery as a decision variable
Model Nature	Low complexity, low precision, linear	Medium complexity, higher precision, nonlinear	High complexity, highest precision, nonlinear
Optimization Techniques[d]	Linear programming or MILP	Nonlinear programming (linearization needed)	Nonlinear programming (linearization needed)
Advantages	Simple, computationally efficient, suitable for large-scale systems	More accurate representation of AEL efficiency variations	Comprehensive analysis considering varying efficiency, thermal dynamics, and heat recovery
Disadvantages	Overly simplistic, may not capture actual system behavior	Increased computational complexity, simplifications or linearization may reduce accuracy	Highest computational complexity, simplifications or linearization may reduce accuracy

[a] EtH relationship refers to the electricity-to-hydrogen production rate correlation.
[b] EtHH relationship denotes the interplay among electricity, heat, and hydrogen production.
[c] *Dependent* means that system efficiency varies with system parameters (input power, temperature, pressure, etc.).
[d] Optimization techniques indicate the resulting decision-making optimization model due to integrating the relevant AEL models.

(iii) IEHHM is most suitable for system-level studies that incorporate thermal effects, enable waste heat recovery, or target co-optimization of hydrogen and heat.

Ultimately, the choice involves a trade-off between model complexity, computational efficiency, and the desired accuracy for the intended application.

3.5. AEL model integration in decision-making optimization of energy systems

The three AEL models reviewed in this paper is only providing foundational representations of AEL device behavior for system-level optimization, each representing distinct levels of modeling granularity. As shown in Fig. 7(a), LEHM and NEHM primarily model the electricity-to-hydrogen (EtH) conversion, in linear and nonlinear manner, respectively; while IEHHM extends this to include heat as a co-product, representing the electricity-to-heat-and-hydrogen (EtHH) process. These models, regardless of their internal complexity, are formulated as a high-level input–output mapping to characterize the AEL device, which facilitates modular integration into broader decision-making optimization frameworks without changing the optimization problem's structure. Once embedded into system-level optimization models, these AEL representations function as device submodels that impose AEL's physical constraints within a larger system architecture. The optimization models of larger systems, as shown in Fig. 7(b), are typically classified based on their uncertainty handling approaches (e.g., deterministic, stochastic), optimization objectives (e.g., economic, reliability, or multi-criteria), and solving techniques (e.g., mathematical programming, heuristic methods).

Notably, these classifications belong to the overall optimization architecture of the energy system, rather than defining new AEL device-level model categories. Each framework typically integrates one of the AEL models (LEHM, NEHM, or IEHHM) as its electrolyzer submodel according to the desired trade-off between modeling accuracy and computational complexity. For instance, a stochastic optimization for a wind-hydrogen system seeking operational tractability may adopt LEHM or linearized NEHM, while multi-energy co-optimization scenarios that leverage waste heat recovery may benefit from IEHHM.

This review systematically focuses on these device-level AEL models (LEHM, NEHM, IEHHM). An overview of their application within various decision-making optimization contexts in energy systems is presented in Section 4, clarifying their practical implementation.

4. Application of AEL models in decision-making optimization

This section presents a critical review of how AEL models are applied in system-level decision-making optimization across various operational and planning aspects within AEL-integrated energy systems. The focus is specifically on studies corresponding to Levels 5 and 6 of the hierarchical framework in Fig. 4. The decision-making entities considered range from AEL owners to operators of complex hybrid energy systems. The literature selection for this review follow specific criteria to ensure relevance and depth: *(i)* the presented electrolyzer models are tailored for the AEL type; *(ii)* publications are primarily drawn from leading peer-reviewed journals in energy systems, hydrogen technology, and chemical engineering, spanning the years 2000 to 2024, to ensure a high standard of research and a comprehensive timeframe. Studies that employed three AEL models without offering novel applications, methodological innovations, or insights relevant to system-level optimization, are specifically excluded; and *(iii)* the primary focus of the selected studies is on decision-making for optimizing the operation and/or planning of individual AEL systems or AEL-integrated energy systems.

Based on these selected publications, the focused system-level applications are categorized into four principal types: economic operation, grid services, heat recovery management, and capacity planning. In the following subsections, each representing an application area, the critical analysis of how different AEL models have been employed in each application is provided, discussing their implications for optimization strategies and outcomes, and highlighting key research trends and challenges.

4.1. Economic operation

The economic operation application involves creating economic benefits of AELs via optimizing their operation schedule for AEL operators, co-scheduling within AEL-integrated hybrid plants, and even

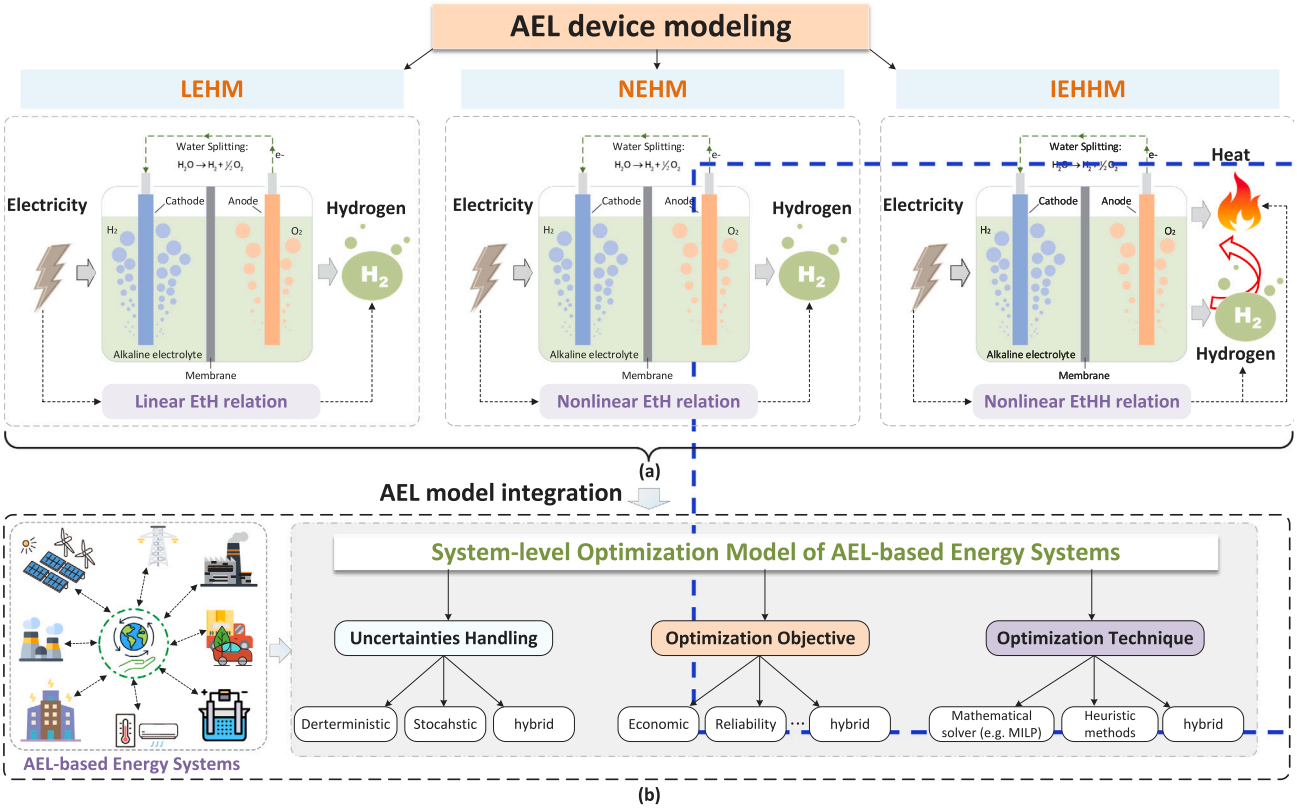

Fig. 7. AEL model integration with decision-making optimization model of energy systems: (a) AEL three models and corresponding energy conversion relationship (EtH or EtHH); (b) the classification of system-level decision-making optimization model.

energy systems (e.g. microgrids) to maximize the system's profits (or minimize the system operation cost), considering both energy price fluctuations, renewables generation and demands. It typically includes economic arbitrage for independent AEL and AEL-integrated hybrid system operators (e.g. hybrid wind-hydrogen systems), and economic dispatch of energy systems such as microgrids and power grids. Notably, this application does not include added-value revenues which typically include additional revenues from AEL's offering grid service and heat recovery. These revenue streams will be explained in other applications.

The energy arbitrage of independent AEL operators is achieved through managing the AEL to generate profits by buying electricity to produce hydrogen at low electricity prices (lower than the hydrogen sale price) and stopping AEL operation at high electricity prices (higher than the hydrogen sale price). In the case of hybrid systems that integrates AELs and renewable power plants, the arbitrage chance of the hybrid plants will be improved due to integrating the revenue stream of renewable power. In this case, the energy arbitrage is exploited by: prior to using renewable power to produce hydrogen at low electricity prices and buying electricity to produce hydrogen if renewables deficit; at high electricity prices, prior to selling renewables power to grids while producing hydrogen if the remaining power is available otherwise stopping AEL. When it comes to the economic dispatch of AEL-integrated energy systems, the economic operation management of AELs will become more complex. In such cases, economic co-scheduling between AELs and other facilities such as renewables power plants and storages, needs to be implemented to optimize multifold revenue streams thereby minimizing the system operation cost. The economic operation is formulated as an optimization problem to maximize the profit of the independent AEL owners and hybrid plant owners or to minimize the cost of running the AEL-integrated energy system from the perspective of the independent system operators. The contribution from AELs via taking advantage of the electricity and hydrogen price volatility to the objective cost function is expressed as follows:

$$C_{ea} = \sum_{t=1}^{T_h} \left(\lambda_t^e P_{AEL} \Delta t + c^{su} b_t - \lambda^h \dot{m}_{\mathrm{H_2}} \Delta t \right) \tag{50}$$

where λ_t^e is the electricity price at time t; b_t is a binary variable for representing the start-up of AELs i.e. switching from shut down to production or standby; c^{su} is the start-up cost (€); λ^h denotes the hydrogen selling price, which is usually assumed to be constant; Δt is the time interval; T_h denotes the scheduling horizon.

Eq. (50) represents the operation cost of AEL, which is equal to the cost of buying electricity and AEL start-up minus the revenue of selling hydrogen. Minimization of this cost directly forms the objective function for economic arbitrage of independent AEL owners [95], but it can be changed in different extends e.g. removing the start-up cost term when ignoring the state-switching of AELs. While in the case of economic arbitrage of hybrid plants and economic dispatch of energy systems, the cost Eq. (50) offers a cost contribution from AEL operation to the total objective cost function.

The LEHM has long been a preferred option for economic analysis of AEL systems, primarily due to its simplicity and compatibility with linear and MILP formulations. In early studies, it offers a practical way to model large-scale systems or explore complex operation strategies without overly computational burden. LEHM is widely used to assess wind-hydrogen hybrid systems, especially for modeling market participation and optimal system planning [64]. In microgrid studies, it supports scheduling strategy development under operational constraints such as frequency regulation [65], and in multi-objective frameworks, it facilitates optimization across costs, emissions, and grid services [67]. Its application has also extended to hydrogen logistics planning [66], demand-response scheduling for fueling stations [68], and operation of large AEL clusters within power systems [69]. Despite its advantages, LEHM is limited by its assumption of constant

Table 4
Comparison of the literature on economic operation applications with respect to AEL modeling and optimization techniques.

Study	AEL model	Model approximation	AEL state-switching[a]	Objective function[b]	Optimization technique	Uncertainty	Interval/ horizon
[64]	LEHM	None	On/Off	Obj 2	LP	Deterministic	1 h/ 48 h
[65]	LEHM	None	On/Off	Obj 3	MILP (CPLEX-solved)	Deterministic	12 min/ 24 h
[66]	LEHM	None	None	Obj 2	MILP	Deterministic	1 month/ 1 year
[67]	LEHM	None	On/Off	Obj 3	MILP (MATLAB-solved)	Deterministic	15 min/ 2 weeks
[68]	LEHM	None	None	Obj 1	NP (CIP-NTR-solved)[c]	Deterministic	1 h/ 1 week
[69]	LEHM	None	On/STB/Off	Obj 3	MILP (Gurobi-solved)	Deterministic	1 h/ 24 h
[15]	NEHM	Linear Eq. (26)	On/STB/Off	Obj 2	MILP (Gurobi-solved)	Deterministic	1 h/ 1 year
[97]	NEHM	None	On/Off	Obj 2	Artificial bee colony	Deterministic	1 h/ 24 h
[82]	NEHM	PWL Eq. (28)	None	Obj 2	MILP	Deterministic	1 h/ 72 h
[81]	NEHM	PWL Eq. (28), Quadratic Eq. (27)	On/STB/Off	Obj 2	MILP, MISOCP[d], solved by Gurobi	Deterministic/ Stochastic	1 h/ 24 h
[80]	NEHM	PWL Eq. (29)	On/STB/Off	Obj 2	DRCCP→[e] MILP, solved by Gurobi	Robust chance-constrained	1 h/ 24 h
[98]	NEHM	Quadratic Eq. (30)	On/Off	Obj 2	MINLP (BARO-solved)	Deterministic	15 min/ 24 h
[99]	NEHM	None	None	Obj 3	DDPG[f]	Deterministic	1 h/ 24 h
[100]	NEHM	None	None	Obj 3	Harmony Search	Stochastic	1 h/ 24 h
[86]	NEHM	PWL	On/Off	Obj 3	MINLP→MILP (Gurobi-solved)	Stochastic	15 min/ 1 week
[101]	NEHM	None	On/STB/Off	Obj 3	Beluga whale optimization	Deterministic	1 h/ 24 h
[93]	IEHHM	Linear	On/STB/Off	Obj 2	MILP	Deterministic	1 h/ 24 h

[a] *(1) None:* AEL always works without no state-switching; *(2) On/Off:* AELs switch between the production (on) mode and shut-down (off) mode. *(3) On/STB/Off:* AELs switch among the on mode, standby mode (STB) and off mode.
[b] *(1) Obj 1:* refers to economic energy arbitrage for independent hydrogen system (e.g. only AELs, AEL+tank, AELs+tank+fuel cells.); *(2) Obj 2:* refers to economic energy arbitrage for on/off-grid hybrid renewable-hydrogen plants (e.g. wind-hydrogen systems); *(3) Obj 3* refers to economic dispatch within AEL-integrated energy systems (e.g. microgrids and power systems).
[c] CIP-NTR means the combined interior point nonlinear programming and newton trust region solution mechanism.
[d] MISOCP is the mixed-integer second-order cone programming.
[e] DRCCP means distributionally robust chance-constrained programming. The symbol → means transforming the original optimization into another one.
[f] DDPG is the deep deterministic policy gradient algorithm.

efficiency. While this assumption enables fast computation, it often fails to reflect realistic performance, especially under partial load or transient operating conditions. This mismatch between simplicity and operational realism has motivated a shift toward NEHM, which capture AEL's efficiency variations more accurately and support improved decision-making.

NEHM considers AEL's characteristics of polarization curve and dynamic efficiency, enabling more realistic representations of AEL behavior in operation optimization. This modeling feature is particularly important in wind-electrolyzer systems, where power inputs are highly fluctuating. To manage the computational burden of nonlinearity, various approximation methods (discussed in Section 3.2.2) have been adopted, such as linearization and PWL fitting. These approaches support the use of MILP solvers while preserving key efficiency characteristics to different degrees [15,82]. Simpler approximations are often favored in short-term scheduling, while higher-order methods, including quadratic or robust formulations, are applied when uncertainty or system complexity requires greater accuracy [80,81]. These frameworks have demonstrated improvements in cost efficiency and system reliability under renewable and market volatility.

Several studies have explored alternatives to traditional mathematical programming. Fuzzy control [97] and metaheuristic algorithms [101] have been applied to NEHM-integrated optimization models, particularly for real-time or non-convex problems. NEHM has also been integrated into multi-objective optimization to evaluate trade-offs between economic value and environmental impact, such as in solar-AEL systems [98] or wind-based hybrid designs [82]. In off-grid and complex hybrid systems, NEHM supports reinforcement learning-based dispatch (e.g., deep deterministic policy gradient algorithm) [99], scenario-based uncertainty modeling in microgrids [86], and hydrogen-fuel cell integration [100]. These diverse applications prove NEHM's adaptability, though its computational cost remains a constraint in large-scale optimization problems.

Compared to LEHM and NEHM, the IEHHM provides a broader view by modeling both thermal and electrochemical dynamics. It enables improving energy utilization and unlock added economic value by accounting for waste heat recovery. Recent work has demonstrated the application of IEHHM in wind-electrolyzer systems, capturing temperature effects on efficiency and jointly scheduling hydrogen and heat flows [93]. These models incorporate switching of operational modes, temperature-dependent performance, and heat exchange dynamics, offering a more complete representation of AEL behavior in energy management. However, IEHHM has yet to be widely used in dispatch studies. Its main drawback lies in model complexity. Including thermal dynamics introduces additional variables and nonlinearities, which are difficult to handle in long time-horizon or multi-node energy system optimization. As a result, current applications are limited to small-scale case studies or rely on simplifications. Despite these challenges, the potential for IEHHM to unlock greater economic value from AELs, especially when integrated with district heating or industrial heat demand, still suggests an important future direction for research in AEL economic operation.

Table 4 provides a comparative overview of the reviewed literature on AEL models in economic operation, revealing several key trends and critical insights. A clear evolution toward models with higher physical accuracy is evident, with NEHM now being the most prevalent choice,

utilized in over half of the analyzed studies. This reflects a growing recognition that capturing variable AEL efficiency is crucial for accurate dispatch optimization. To manage the inherent nonlinearity of NEHM, approximation techniques like piecewise linearization and quadratic fitting have become standard practice, trying to balance solution accuracy with computational efficiency. However, the reliance on these approximations means that many NEHM-based optimization models still necessitate advanced solvers or heuristic algorithms to handle the residual complexity, particularly for large-scale or real-time applications. In addition, it aslo indicates the predominance of deterministic optimization frameworks for dealing with economic operation, though recent studies have introduced stochastic and robust methods to address renewable variability and market uncertainties. Furthermore, the inclusion of AEL state-switching (on/off/standby modes) is commonly considered, with binary variables used to represent AEL operation modes and transitions. This better reflects the realistic operational environment of AELs, but increasing complexity to the optimization formulations.

Overall, the analysis of reviewing those studies implies a clear progression toward more detailed AEL models for economic operation. However, several significant challenges remain, particularly in: (1) effectively integrating detailed thermal dynamics (via IEHHM) into scalable operation models; (2) managing diverse uncertainties without compromising tractability, and (3) solving large-scale and potentially non-convex optimization problems arising from high-accuracy AEL representations. Addressing these challenges will be essential for realizing the full economic potential of AEL technologies in future multi-energy systems.

4.2. Grid service

The grid service application explores the feasibility and economic benefits of AELs participating in grid ancillary services, notably frequency regulation services, to balance the grid when supply and demand are mismatched. Recent advancements in AEL technologies have demonstrated AEL's qualified frequency regulation capabilities. Advanced AELs like the pressurized AELs exhibit rapid power up/down-regulation within seconds [14,15,102]. This fast ramping capability makes them capable of providing frequency regulation for grids, as investigated in [7,103]. Depending on the structure of particular electricity markets, the participated markets and frequency regulation products can be different. For example, the Danish case demonstrates that the provided products from AELs could be frequency containment reserve (FCR), automatic frequency restoration reserve (aFRR), manual frequency restoration reserve (mFRR), traded in reserve markets and/or real-time markets (also called balancing markets) [70]. Furthermore, the frequency service provider could be paid via two revenue streams. The first one is the payment of provided reserve capacity for frequency regulation, referred to as capacity revenue or availability payment [104]; while the second one is the payment of activated up/down reserve for frequency regulation in real-time operation, called regulation revenue or performance revenue [70,83]. Providing grid service will bring additional revenue streams and the corresponding revenues will be added to the objective cost function of decision-making optimization models. In the Danish market structure, it can be expressed by Eqs. (51)–(53) [7,70]. While in the PJM market (North America's market) [83], the performance revenue is usually formulated by Eq. (54). The revenue expression can be even simpler when the product is only single i.e. not distinguishing the up/down product, as presented in Eq. (55) [83].

$$C_{gs} = -\left(C_{gs}^{ca} + C_{gs}^{re}\right) \tag{51}$$

$$C_{gs}^{ca} = \sum_{t=1}^{T_h}\left(\lambda_t^{c,up} P_t^{c,up}\Delta t + \lambda_t^{c,dw} P_t^{c,dw}\Delta t\right) \tag{52}$$

$$C_{gs}^{re} = \sum_{t=1}^{T_h}\left(\lambda_t^{r,up} P_t^{r,up}\Delta t + \lambda_t^{r,dw} P_t^{r,dw}\Delta t\right) \tag{53}$$

$$C_{gs}^{re} = \sum_{t=1}^{T_h}\left[\rho\left(P_t^{r,up} + P_t^{r,dw}\right)\Delta t\right] \tag{54}$$

$$C_{gs} = \sum_{t=1}^{T_h}\left(\lambda_t^{c} P_t^{c}\Delta t\right) + \sum_{t=1}^{T_h}\left(\lambda_t^{r} P_t^{r}\Delta t\right) \tag{55}$$

where C_{gs}^{ca} and C_{gs}^{re} represent the capacity revenue and regulation revenue, respectively; The superscript c and r in λ denote the capacity price and regulation price; The superscript c and r in P denote the offered frequency reserve capacity and activated capacity for real-time regulation; The superscript up, dw in λ, P represent the up and down frequency regulation service, respectively.

Due to its computational simplicity, the LEHM has been widely used in early studies on AEL participation in grid services. Its tractable structure allows for straightforward integration into scheduling models, particularly those formulated as linear or MILPs. This has made LEHM a natural choice when co-optimizing electrolyzers with other assets or designing market participation strategies. For example, techno-economic assessments under German market conditions employs LEHM to evaluate the profitability of AELs providing secondary control reserve, emphasizing the influence of system design and operational strategies [105]. In scenarios involving large-scale AEL deployment, such as co-location with EV charging infrastructure, LEHM-based dispatch models have demonstrated the potential of grid service revenues to improve system profitability [104]. As research progresses, LEHM has been integrated into more advanced optimization frameworks that address uncertainty. An example is using chance-constrained stochastic programming to co-optimize energy arbitrage and ancillary service participation in PV-battery-AEL hybrid systems [106]. This enabled profit maximization while accounting for variability in solar power and grid signals. Similarly, studies in the Danish market apply LEHM within market-based models to estimate revenues from different reserve services and assess hydrogen break-even prices under various participation scenarios [7,70].

Nevertheless, LEHM's core assumption of constant efficiency introduces limitations when modeling AELs under dynamic operating conditions, such as those encountered during frequency regulation. This simplification may lead to inaccuracies in estimating hydrogen production or energy use during grid service events, potentially distorting cost assessments and bidding strategies. Thus, while LEHM provides a useful first-order approximation, its fixed-efficiency structure restricts its ability to accurately represent the dynamic behavior required in fast-response grid services.

To address this gap, recent efforts have begun incorporating NEHM into grid service participation. One example applies a piecewise-linear NEHM within a robust cooperative bidding strategy for a wind-electrolysis system [83]. This model enables more accurate hydrogen production estimation under grid services and allows for trade-off analysis between grid service revenue and hydrogen output. While this direction reflects growing interest in higher-accuracy representations, NEHM adoption in this scenario remains limited, due to the increased computational complexity involved in real-time bidding or high-resolution scheduling.

Table 5 summarizes the reviewed studies on AEL modeling for grid service applications. LEHM remains the prevailing choice, primarily due to its simplicity and tractability. Its linear structure facilitates straightforward integration into system-level scheduling and market optimization frameworks, enabling efficient, albeit simplified, assessments of AEL's economic potential in frequency services, including revenue estimation and profitability analysis across various market scenarios. However, this simplicity of AEL dynamics comes at the expense of physical accuracy. Besides, it is revealed that NEHM has only recently appeared, and IEHHM is absent entirely, pointing to notable gaps in representing AEL's key dynamics during grid service provision.

Therefore, based on the literature review analysis, three critical needs emerge : (a) Capturing the efficiency variation and transient behavior of AELs during frequent load changing conditions typical of grid

Table 5
Comparison of the literature on grid service applications with respect to AEL modeling and optimization techniques.

Study	AEL model	AEL state-switching	Objective function	Grid service	Optimization technique	Uncertainty	Interval/ horizon
[105]	LEHM	None	Wind prediction error reduction	Frequency service	Rule-based	N/A	4 s/ 1 year
[104]	LEHM	On/STB	Obj 1	F[1]	MILP (simplex algorithm-solved)	Deterministic	1 h/ 1 year
[106]	LEHM	On/Off	Obj 2	F[2]	MILP (Gurobi-solved)	Chance-constrained stochastic	1 h/ 21 days
[70]	LEHM	None	Obj 2	F[2]	MILP (Gurobi-solved)	Deterministic	1 h/ 3 years
[7]	LEHM	None	Obj 1	F[2]	LP (Gurobi-solved)	Deterministic	1 h/ 3 years
[83]	NEHM (PWL[3])	On/STB	Obj 2	F[2]	robust optimization	Robust	1 h/ 1 year

F[1] refers to the frequency service which only considers the capacity revenue.
F[2] refers to the frequency service which accounts for both the capacity revenue and regulation revenue.
PWL[3] This term means the NEHM model is approximated by a piecewise linearization method.

services; (b) Accounting for thermal effects that may significantly influence AEL performance under repeated activation scenarios, by using IEHHM; (c) Incorporating uncertainty in both resource availability and service activation, as most current models remain deterministic, with few exceptions applying robust or stochastic methods. Particularly, future work should consider integrating more detailed AEL models (e.g. NEHM and IEHHM) into uncertainty-aware optimization frameworks to improve the accuracy and reliability of dispatch outcomes. This would provide a stronger foundation for evaluating the technical feasibility, economic performance, and service potential of AELs in ancillary service markets.

4.3. Heat recovery management

As analyzed in the thermal modeling of Section 3.3, the heat released during the electrolysis process can be extracted via heat exchangers, corresponding to the cooling power $\dot{Q}_{cool}$, to maintain the AEL temperature. This recovered heat presents a valuable opportunity for enhancing system efficiency and creating additional revenue streams by supplying for heat loads or district heating systems (DHSs). The heat recovery management application focuses on optimizing the management of this recovered waste heat generated by AELs during their operation, improving overall system benefits through heat selling or by directly offsetting heating costs. The revenue of selling recovered heat can be added to the objective cost function of decision-optimization models, as expressed by Eq. (56). In addition, the recovered heat could also contribute to cost function reduction by using the recovered heat to supply part of heat loads thereby reducing heating costs.

$$C_{he} = -\sum_{t=1}^{T_h} \lambda_t^{he} \dot{Q}_{cool} \Delta t \tag{56}$$

where λ_t^{he} denotes the price of heat sale; $\dot{Q}_{cool}$ represents the available recovered heat and is subjected to the thermal behavior characterized by the thermal model of AELs.

The IEHHM is the standard choice for modeling AELs in heat recovery studies, due to its ability to capture coupled electrochemical, thermal, and hydrogen production dynamics. Current literature follows two main approaches to leveraging heat recovery for economic benefit: (1) using the recovered heat to meet heat demand and reduce system operating costs; (2) directly accounting for heat revenue by treating it as a marketable product in heat markets.

The first approach is the most common, i.e. using recovered AEL heat to meet existing thermal demands. In distribution networks with high renewable penetration, IEHHM models that are often simplified via multi-segmented linearization (MSL) have been embedded in dispatch strategies to delivery waste heat to district heating systems (DHSs). This has proven effective in enhancing system flexibility, reducing renewables curtailment and operational costs [94]. Experimental validation of IEHHM-based models has also confirmed that temperature strongly affects AEL performance, supporting dispatch strategies where heat recovery improves energy conversion efficiency at the microgrid level [90]. IEHHM has further been used to coordinate AELs with CHP units and hydrogen storage, expanding the feasible operating region of energy systems and enabling additional reductions in fuel consumption and emissions [91]. At the utility scale, scheduling models integrating AEL's thermal and impurity constraints, also based on MSL-approximated IEHHMs, have been shown to increase both operational flexibility and investment return through coordinated multi-physics control [95]. While MSL approximations improve computational tractability, they may introduce errors in capturing nonlinear thermal effects, which can affect dispatch outcomes in high time-resolution conditions.

Other studies focus on the second approach i.e. treating recovered heat as a co-product, adding it directly to the revenue stream. This often requires more advanced control strategies. Model Predictive Control (MPC) frameworks have been developed to manage AEL-DHS interactions, with IEHHM models integrated either in simplified single-segmented linear (SSL) form or in full nonlinear detail. Early studies using SSL approximations have shown that even moderate heat recovery (e.g., supplying 10% of DHS demand) could be economically valuable without compromising AEL efficiency [96]. More recent work has implemented detailed IEHHM models without linearization, directly within MPC optimization for hydrogen-based multi-energy microgrids [88,89]. These studies integrate heat revenue into the objective function and employ advanced MPC algorithms to ensure AEL's operational feasibility and maximize economic benefits. This shift toward using unapproximated IEHHM suggests the direction of developing advanced solving algorithms to handle detailed multiphysics models efficiently.

Table 6 provides a summary of the reviewed literature on heat recovery applications. All reviewed studies rely on IEHHM, confirming its essential role in modeling the thermal behavior of AELs. Most of them adopt MSL or SSL approximations to improve tractability, especially in large-scale or real-time contexts. However, the increasing adoption of direct nonlinear MPC implementations indicates that high-accuracy modeling is becoming more feasible in practice. This development is important for improving the accuracy of heat recovery assessments and avoiding the limitations of simplified models.

One notable limitation across the literature is the universal reliance on deterministic formulations. The effectiveness of AEL heat recovery can vary significantly under uncertain thermal demands, electricity prices, or renewable inputs. Most of the reviewed studies do

Table 6
Comparison of the literature on heat recovery management applications with respect to AEL modeling and optimization techniques.

Study	AEL model	Model approximation[a]	AEL state-switching	Objective function	Heat recovered contribution[b]	Optimization technique	Interval/ horizon
[94]	IEHHM	MSL	None	Obj 3	Indirect	MIQCP (Robust)	1 h/ 24 h
[90]	IEHHM	MSL	None	Optimal state tracking	Indirect	MIQP (Deterministic)	1h/ 24 h
[91]	IEHHM	MSL	None	Obj 3	Indirect	MILP (Deterministic)	1 h/ 24 h
[95]	IEHHM	MSL	On/STB/OFF	Obj 1	Indirect	MILP (Deterministic)	15 min/ 24 h
[96]	IEHHM	SSL	On/OFF	Obj 3	Direct	MILP (Deterministic)	1 h/ 24 h
[88]	IEHHM	None	On/OFF	Obj 3	Direct	MPC-MILP (Deterministic)	1 h/ 24 h
[89]	IEHHM	None	On/OFF	Obj 3	Direct	MPC-MILP (Deterministic)	1 h/ 24 h

[a] The model approximation includes two types: (1) MSL is multi-segmented linearization, referring to using multiple segmented linear planes to approximate the nonlinear plane characterized by the inherent nonlinearity of AEL; (2) SSL is single -segmented linearization, which means using only one linear plane to conduct the approximation.
[b] This term involves two types: (1) Direct means considering the revenue of recovered heat sale and being directly added into the objective cost function; (2) Indirect means using recovered heat to supply heat loads, indirectly offsetting the heating cost.

not account for these uncertainties, except that only one considers the uncertainty of renewable power. Thus, future work should further explore uncertainty-aware optimization methods (e.g., stochastic or robust methods) in conjunction with IEHHM-based modeling. Incorporating uncertainty would enable more resilient and realistic strategies to manage AEL heat recovery in complex and variable energy environments.

4.4. Capacity configuration

The capacity configuration application focuses on optimizing the capacity configuration and design of AELs-integrated hybrid energy systems (e.g., microgrids, hybrid renewables-battery-hydrogen systems). The goal is typically to find the optimal sizes of electrolyzers and other devices (e.g., batteries, wind generators) to minimize system costs (or maximize system profits), meet energy needs, maximize hydrogen production, and so on. Depending on the focused systems/projects and their particular purposes, the objective function of capacity configuration could be different. Whereas, there are several common techno-economic indicators: (i) financial indicators: present value (NPV), net present cost (NPC), life cycle cost (LCC), of single and multiple devices within energy systems, as well as, levelized cost of hydrogen (LCOH) and levelized cost of energy (LCOE) of energy systems, etc.; (ii) non-financial indicators: loss of power supply probability (LPSP), hydrogen production, carbon emission (CE), etc. Furthermore, these indicators usually include many items and sub-items, particularly, their calculation is quite distinct depending on particular energy systems and purposes. It is thus hard to give a general formulation for characterizing the objective function suitable to all of the studies.

Given the long time-horizon (e.g. yearly resolution) of capacity planning and the need to accurately reflect efficiency under varying loads, NEHMs are widely adopted. They allow planners to account for part-load behavior and nonlinear energy conversion characteristic in AEL systems, especially when coupled with variable renewable inputs. However, integrating NEHM, even in approximated forms, into optimization frameworks introduces significant complexity, particularly when combined with multiple objectives or uncertain inputs. In off-grid systems, for example, NEHM-based models have been integrated with heuristic solvers such as strength pareto evolutionary algorithms to evaluate trade-offs across system cost, emissions, and energy balance [78]. More advanced leader–follower frameworks combine linearized NEHM dispatch models in the lower layer with upper-layer genetic algorithms for sizing [75,76]. These frameworks are further used to clarify the impact of component degradation, forecast uncertainty, and operational strategies on sizing results. Other works fit NEHM using polynomials and apply particle swarm optimization to minimize LCOE in remote hybrid systems [85].

At larger scales, NEHM has been incorporated into planning models for national infrastructure. For instance, coordinated sizing of HVDC lines and power-to-hydrogen supply chains has been addressed using piecewise NEHM approximations within distributionally robust chance-constrained programming frameworks [84]. These models evaluate AEL sizing alongside broader infrastructure under renewable uncertainty. Offshore wind systems, by contrast, have adopted convex programs with quadratically approximated NEHM to optimize hybrid hydrogen-battery storage [110]. In both cases, model approximation such as piecewise, polynomial, quadratic, is essential to maintain tractability across long-time horizons.

While NEHM dominates recent work, LEHMs are still used where computational efficiency or solver compatibility is prioritized. Off-grid system designs often apply LEHMs in NSGA-II frameworks to balance system reliability and cost without the burden of nonlinear modeling [107]. They are also used to co-optimize energy dumping, hydrogen shortfall, and emissions [71]. In addition, LEHMs are also employed in long-term NPV optimization for PV-battery-electrolyzer systems [72], and in multi-stakeholder power-to-ammonia systems to coordinate capacity sizing and pricing through two-stage decomposition [108]. Despite known simplifications, LEHM's tractability remains an advantage in certain planning contexts.

Though less common, IEHHMs have begun to appear in capacity planning where thermal behavior and heat integration are relevant. In wind-PV-hydrogen systems, full IEHHMs have been used to assess operational reliability and production stability with coupled thermal-electric dynamics [111]. Single-segment linearized IEHHMs are also used in planning seasonal hydrogen storage within an electricity–hydrogen integrated energy system, employing a hybrid stochastic-robust optimization framework [92]. These efforts highlight that, despite their complexity, IEHHMs can offer value in systems where thermal characteristics significantly affect sizing decisions.

Table 7 summarizes these studies and highlights how modeling choice impacts optimization strategy. Linearized NEHMs are most common, offering a trade-off between accuracy and solvability. When problem complexity grows due to multiphysics coupling or uncertainty, heuristic solvers (e.g., GA, PSO, NSGA-II) and decomposition methods (e.g., nested column-and-constraint generation) are often employed. LEHMs remain useful when compatibility with MILP solvers is required, particularly in early-stage or investor-focused planning.

Table 7
Comparison of the literature on capacity configuration applications with respect to AEL modeling and optimization techniques.

Study	AEL model	Model approxi-mation	AEL state-switching	Objective function	Optimization technique	Uncertainty	Interval/ horizon
[107]	LEHM	None	None	Min. system cost + LPSP	NSGAII[a]	Deterministic	1 h/ 1 year
[71]	LEHM	None	On/Off	Multi-objectives[b]	Iterative method	Deterministic	1 h/ 1 year
[72]	LEHM	None	On/STB/Off	Optimized NPV	MILP (Gurobi-solved)	Deterministic	1 h/ 1 year
[108]	LEHM	None	None	Min. system cost	MINLP, solved by two-stage decomposed method	Robust	1 h/ 1 year
[78]	NEHM	Linear Eq. (25)	None	Min. NPC+LPSP+CE	SPEA[c]	Deterministic	1 h/ 1 year
[76]	NEHM	Linear Eq. (24)	On/Off	Min. system cost[d]	GA+MILP	Robust	1 h/ 1 year
[75]	NEHM	Linear Eq. (24)	On/Off	Min. system cost	GA+MILP	Robust	1 h/ 1 year
[85]	NEHM	Polynomial fitted	On/Off	Min. LCOE	PSO	Deterministic	1 h/ 1 year
[84]	NEHM	PWL	On/Off	Min. system cost	DRCCP→ MIQCP (CPLEX-solved)	DRCCP	1 h/ 1 year
[109]	NEHM	None	On/STB	Min. grid-exchanged power	Analytical optimization method	Deterministic	1 h/ 1 year
[110]	NEHM	Quadratic	On/Off	Min. system cost	NP (relaxation into convex form, solved by CVX)	Deterministic	1 h/ 1 year
[111]	IEHHM	None	None	Max. hydrogen production	Imperial competitive colony	Deterministic	1 h/ 1 week
[92]	IEHHM	SSL	On/Off	Min. system cost	NP[e] (nested-C&CG)	Stochastic & robust	1 h/ 1 year

[a] NSGAII means non-dominated sorting genetic algorithm.
[b] The multiple objectives of this study consist of minimizing LCOH, total hydrogen deficit, energy dump possibility, maximizing carbon emissions avoided and natural gas preserved.
[c] SPEA means the strength pareto evolutionary algorithm.
[d] The constitution of the system cost can be different depending on particular publications, typically including initial capital or investment cost, operation and maintenance cost, and replacement cost, etc., minus the diverse revenue streams.
[e] NP means nonlinear programming, where the solved nested-C&CG method refers to nested column-and-constraint generation.

Although still limited, the use of IEHHM reflects a growing research interest in heat-coupled system optimization. Many studies also include AEL state-switching (e.g. on, off and standby) in the modeling, improving accuracy and supporting feasible dispatch strategies.

Overall, the analysis of the literature review reflects a shift toward more detailed, uncertainty-aware frameworks operating at hourly resolution over long time horizons. This trend aligns AEL planning with broader long-term energy system planning models used for investment decision-making. However, challenges remain in developing efficient approaches that combine physical accuracy, uncertainty handling, and computational tractability within a unified optimization framework.

5. Discussion

The previous sections have synthesized existing AEL models and their applications across system-level decision-making scenarios. This section expands the review by offering a systematic discussion to comparatively summarize key characteristics of each model, current limitations, and prospective advancements. The aim is to highlight the contributions of existing modeling methods, further identify research gaps guide future efforts toward more accurate, efficient, and advanced AEL modeling strategies.

5.1. Summary remarks

This review identifies a variety of system-level AEL modeling approaches based on an analysis of over 100 peer-reviewed studies, also highlighting their roles in optimizing decision-making across four key applications: economic operation, grid services, heat recovery management, and capacity planning.

LEHMs, characterized by their simplicity and computational efficiency, have been prevalent in initial explorations of AEL economic viability and large-scale system planning. They offer a convenient way to represent AELs as simple energy converters with fixed efficiency, enabling the formulation of optimization problems as LP or MILP models that are readily solvable by commercial solvers. However, this simplified approach comes at the cost of neglecting the dynamic efficiency variations inherent to AELs. This oversimplification can lead to inaccurate estimations of hydrogen production and suboptimal operational decisions, potentially resulting in hydrogen safety issues. As the field progresses, there is a growing recognition of the need for more accurate and realistic models.

NEHMs offer a significant advancement by incorporating efficiency variations based on the AEL polarization curve, capturing the impact of operational parameters on system performance. This increased accuracy enables more informed decision-making, leading to more efficient and profitable AEL operation. However, this advantage is accompanied by the challenge of nonlinearity. Integrating NEHMs into optimization frameworks often necessitates the use of nonlinear programming techniques, which can be computationally expensive. To address this, researchers have employed various approximation methods, such as linearization and quadratic fitting, to transform the nonlinear problem into a more tractable form, allowing for the use of solvers like Gurobi

and CPLEX. While these approximations provide a compromise between accuracy and computational efficiency, they inevitably introduce some degree of error.

Furthermore, IEHHMs represent the most comprehensive modeling approach, capturing the coupled relationship between electricity, heat, and hydrogen production. The key advancement of this model lies in the incorporation of detailed thermal dynamics, allowing for a more realistic representation of AEL performance by accounting for the impact of operating temperature on efficiency and hydrogen production. This thermal dynamics integration enables the exploration of thermal management strategies to optimize AEL performance and unlock additional operational flexibility. Specifically, IEHHMs enable the co-optimization of both hydrogen production and waste heat recovery, leading to enhanced system efficiency and economic benefits, particularly in integrated energy systems where waste heat can be utilized for heating purposes or sold to external consumers. However, this comprehensive representation comes at the cost of significant computational complexity. The strong nonlinearity of IEHHMs often requires sophisticated solving techniques, such as MSL or MPC algorithms. While these methods can effectively address the optimization challenge, they are computationally demanding, potentially limiting their applicability to larger-scale systems and necessitating further research into computationally efficient solutions.

Overall, the three models reflect varying levels of detail in representing the multi-physics and energy conversion assumption of AEL systems. As shown in Fig. 8(a), the LEHM assumes a linear relationship between electricity input and hydrogen output, exhibiting a constant conversion efficiency that is typically in the range of 60%–70% [65,67,68,105]. In contrast, the NEHM captures a nonlinear electricity-to-hydrogen relationship and reflects variable efficiency, as illustrated in Fig. 8(b). This relationship is affected by operating temperature which is assumed to be fixed in this model. Different from prior two models, Fig. 8(c) shows the IEHHM incorporates not only the electricity-to-hydrogen conversion but also thermal effects, modeling the nonlinear electricity-to-heat-hydrogen coupling. Unlike NEHM, the IEHHM effectively includes temperature dynamics explicitly rather than assuming it to be constant. Both NEHM and IEHHM can capture efficiency variations which is commonly within an operational range of 60%–80% [82,83,89,94], depending on operational conditions such as input power and operating temperature.

Different AEL models also influence the choice of optimization techniques employed for decision-making studies in energy systems. The linear nature of LEHMs readily accommodates LP or MILP formulations, while NEHMs often necessitate nonlinear programming approaches. The complex nature of IEHHMs often requires tailored solving methods like MSL or MPC-based algorithms. As shown in Tables 4 to 7, the literature demonstrates a diverse array of optimization techniques applied to AEL-related system's decision-making problems. This reflects the need for specialized methods to address the distinct challenges posed by different models and application requirements. Therefore, the choice of AEL model needs a trade-off between model accuracy and computational efficiency by analyzing the requirements of intended applications. Fig. 9(a) summarizes the current distribution of each model's usage across system-level decision-making applications. NEHM is the most frequently adopted (42% of studies), followed by LEHM (35%), and then IEHHM (23%). Fig. 9(b) further provides a more detailed view of the distribution of model usage within specific application areas. It reveals the dominance of IEHHM in heat recovery studies and LEHM in grid service, as well as the preference of NEHM in economic operation and capacity planning.

5.2. Future development

While significant progress has been made in the development and application of AEL models, several cross-cutting limitations continue to constrain their broader impact in energy systems optimization. The current modeling is predominantly challenged by: (1) the limited application scope of high-accuracy models such as IEHHMs beyond thermal use cases; (2) insufficient treatment of critical aspects, particularly degradation mechanisms and BOP dynamics; and (3) computational bottlenecks that hinder the deployment of nonlinear models like NEHM and IEHHM in large-scale decision-making problems. These challenges reflects the need for more holistic, scalable, and computationally efficient AEL modeling frameworks. To address these challenges, several promising directions for advancing AEL modeling in decision-making optimization are worth further exploration:

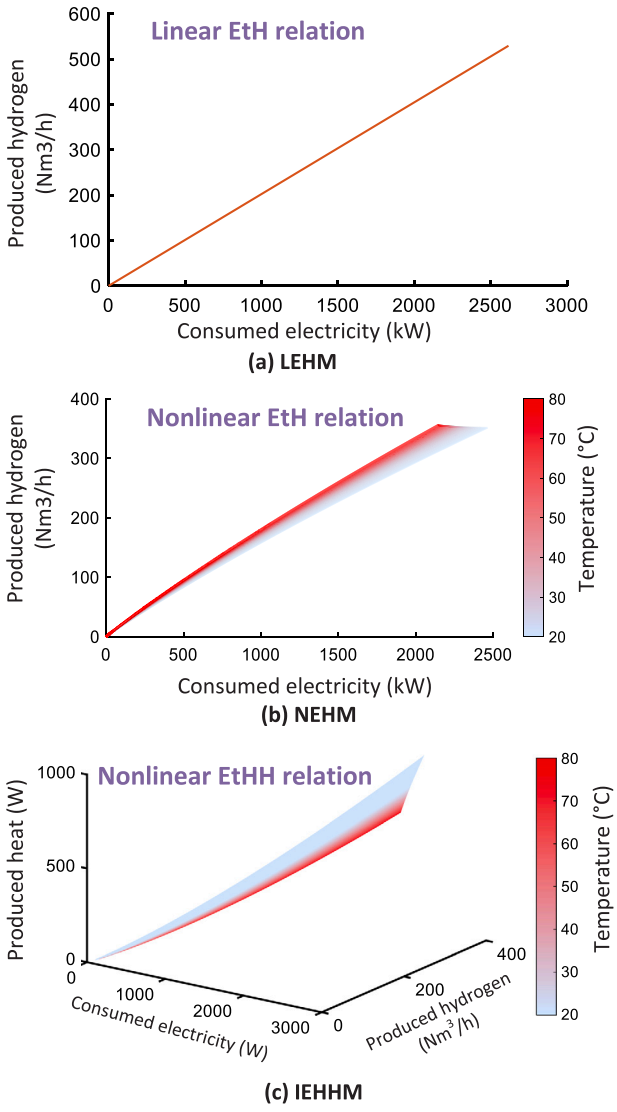

Fig. 8. Comparative energy conversion characteristics of various AEL models using literature-based data [23,89]: (a) LEHM; (b) NEHM; (c) IEHHM.

(1) **Broader exploration of IEHHM applications:** The reviewed literature reveals a significant gap in the utilization of IEHHMs for applications beyond heat recovery management. While IEHHMs offer the most comprehensive approach by capturing the coupled relationship between electricity, heat, and hydrogen production, their application in the reviewed literature has been limited. Future research should explore the potential of IEHHMs to optimize AEL operation across a wider range of applications, particularly in grid services and capacity configuration, where the thermal dynamics of AELs can significantly impact system performance and economic viability.

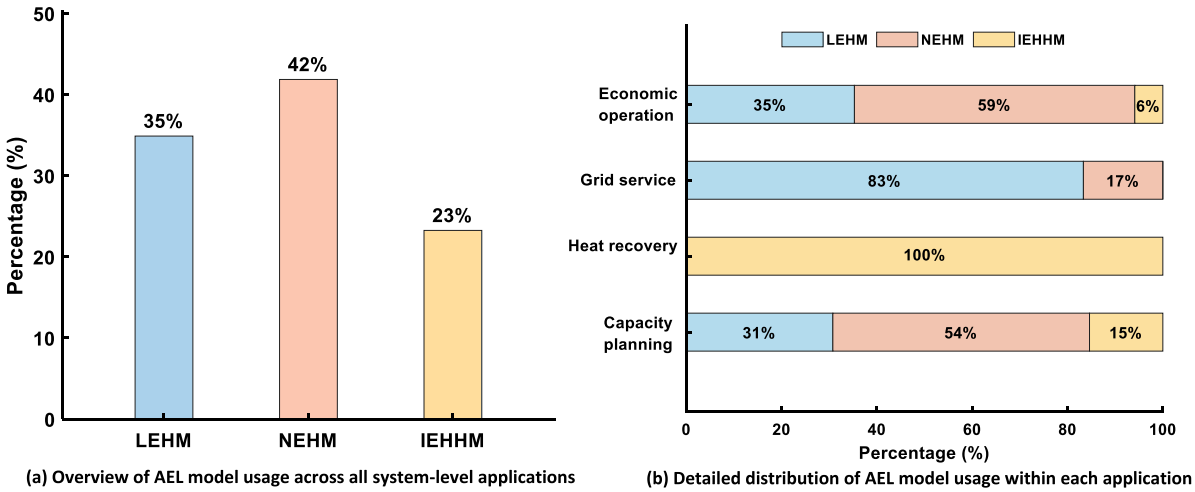

Fig. 9. Distribution of AEL model usage across system-level decision-making optimization studies: (a) Overall model usage percentage; (b) Model usage within each application.

(2) **Comprehensive degradation modeling:** Most of the existing AEL models do not consider their degradation phenomenon. Several relevant studies [76,79,85,96] only offer simplified approaches to modeling AEL degradation, often relying on operational hour limitations, fixed degradation costs, or basic voltage aging terms. Future research should prioritize developing more comprehensive and accurate degradation models for AELs, incorporating factors such as operating time, on/off cycling, input power fluctuations, and temperature variations. Integrating these models into decision-making optimization frameworks would enable more reliable long-term assessments of AEL performance and economic viability, particularly for systems operating with intermittent renewable energy inputs.

(3) **Modeling BOP characteristics and impacts:** Current AEL models often neglect the detailed characteristics and operational constraints of BOP components within AEL systems, primarily focusing on cell and stack characteristics. Future model development should incorporate BOP components and relevant technical constraints, such as pressure limitations, electrolyte dynamics, and gas purity considerations. This integration would enable a more realistic representation of AEL operation, leading to more effective and feasible optimization strategies. Additionally, incorporating BOP control strategies, such as pressure management and electrolyte circulation, into decision-making optimization frameworks could enable the simultaneous optimization of both AEL core operation and BOP control for maximizing system efficiency, reliability, and economic benefits.

(4) **Efficient modeling of large-scale AEL deployments:** The reviewed studies often rely on simplified models for large-scale AEL plants, assuming negligible differences among stacks, and scaling up from single-cell or stack values by multiplying the number of cells or stacks. This simplification overlooks the potential for optimizing the operation of individual AEL units within a plant and can lead to inaccuracies in representing realistic operational characteristics. Future advancements should focus on modeling large-scale AEL plants with multiple electrolyzer units while maintaining computational efficiency. This could involve developing reduced-order models, clustering techniques, or other aggregation methods that balance accuracy and computational burden for effective optimization of large-scale AEL deployments.

(5) **Exploring AEL model applications for comprehensive grid support:** The current emphasis on frequency regulation as the primary grid service provided by AELs overlooks their potential contributions to other essential grid support functions. The next direction could focus on investigating the application of AEL models in optimizing AEL participation in broader grid support, such as voltage support, congestion management, peak shaving, and renewable energy integration. This exploration would enable a more holistic and multifaceted utilization of AELs to enhance grid stability, reliability, and flexibility.

(6) **Advanced computational techniques:** Integrating more detailed AEL models like IEHHMs into decision-making optimization poses significant computational challenges, further amplified by large-scale AEL plant integration and uncertainties in energy systems. To fully leverage the benefits of these sophisticated models and explore complex energy system scenarios, future research should investigate advanced and time-saving computational algorithms. One promising solution is utilizing artificial intelligence and machine learning algorithms, especially investigating their integration with combinatorial optimization techniques.

6. Conclusion

This paper presents a comprehensive review of AEL modeling approaches and their applications in system-level decision-making optimization within energy systems. Building upon a holistic analysis of hierarchical AEL research, this review reveals distinct modeling requirements across different levels of AEL system analysis, highlighting the need for varying granularities and timeframes. Most importantly, the review, focusing on the system-level optimization analysis, systematically categorizes and summarizes existing AEL models into three primary types: LEHMs, NEHMs, and IEHHMs. These models are further analyzed and compared based on their system representation, efficiency characteristics, thermal dynamics considerations, and applicable optimization techniques. The review then critically examines the application of these models across four key decision-making areas: economic operation, grid service provision, heat recovery management, and capacity configuration.

The comparative analysis of different AEL models and applications reveals a distinct evolution in AEL modeling for decision-making optimization, driven by a growing emphasis on capturing the complex dynamics of AEL operation and maximizing their value within energy systems. While simpler LEHMs remain useful for initial assessments and large-scale planning, the reviewed literature demonstrates a clear shift toward more sophisticated NEHMs and IEHHMs to achieve greater accuracy and represent the variable efficiency and coupled energy interactions inherent to AELs. This trend is evident across all four application areas, with NEHMs now prevalent in economic operation and capacity configuration studies, and IEHHMs dominating heat recovery management research. Moreover, the widespread incorporation of

AEL state-switching capabilities highlights the importance of modeling operational flexibility for realistic assessments.

However, several critical research gaps remain. Future research should prioritize a broader exploration of IEHHM applications beyond heat recovery management, expanding the role of AELs in diverse grid services, developing degradation models, and incorporating detailed BOP characteristics and relevant constraints. Additionally, efficient modeling techniques for large-scale AEL deployments and the investigation of advanced computational algorithms, particularly leveraging artificial intelligence and machine learning, are crucial for advancing the field. Addressing these research directions will pave the way for more accurate, robust, and computationally tractable AEL models, enabling their effective integration into future energy systems.

By comprehensively reviewing various AEL models and analyzing their implications for system-level decision-making optimization, this work provides practical guidance for selecting appropriate AEL models for stakeholders, especially engaged in optimizing the design and operation of hydrogen-integrated energy systems. For beginners, such as students or early-stage researchers, it offers a foundational understanding of model types, their characteristics, and trade-offs, while explicitly guiding model selection based on specific application needs. For researchers in the field, the review also informs future investigations by identifying key challenges (e.g., degradation modeling and computational bottlenecks) and emerging trends in AEL integration. Industry practitioners, including energy system planners, hydrogen project developers, and grid service designers, may benefit from the model-to-application mapping and accompanying insights into how model accuracy influences optimization strategies, investment planning, and integration with thermal or ancillary energy systems.

Declaration of competing interest

The authors declare that they have no known competing financial interests or personal relationships that could have appeared to influence the work reported in this paper.

Acknowledgments

The research work shown in this paper has received funding from TenneT TSO B.V. within the research project on “Adaptive fast active power control for stabilization of multi-converter dynamics in offshore electrical energy-hydrogen hubs - FUTURE SYSTEM”. It reflects only the authors’ views, and the aforesaid organization is not responsible for any use that may be made of the paper’s content.

Appendix. Voltage efficiency

The voltage efficiency is defined as the ratio between the thermoneutral voltage and cell voltage, as expressed by Eq. (A.1). The thermoneutral voltage U_{tn} is the minimum voltage required for low-temperature electrolysis to occur without heat integration, at which the electrolyzer cell neither generates nor absorbs heat [6]. It can be calculated by Eqs. (A.2)–(A.8). Note that according to the physical definition of the enthalpy change ΔH of the electrolysis reaction, it satisfies $\Delta H = 3600 M_{\mathrm{H}_2} \cdot HHV$. Accordingly, by substituting Eq. (A.2) into Eq. (A.1), the voltage efficiency can be rewritten as Eq. (A.9). The relation shown in Eq. (11) is therefore proven.

$$\eta_v = \frac{U_{tn}}{U_{cell}} \tag{A.1}$$

$$U_{tn} = \frac{\Delta H}{zF} \approx U_{HHV} + \frac{\phi}{zF} \cdot Y \tag{A.2}$$

$$U_{HHV} = 1.4756 + 2.252 \times 10^{-4} T + 1.52 \times 10^{-8} T^2 \tag{A.3}$$

$$\phi = 1.5 \frac{P_\omega}{P - P_\omega} \tag{A.4}$$

$$P_\omega = e^{\left(0.01621 - 0.138\ m + 0.1933\sqrt{m} + 1.024 \ln P_\omega^*\right)} \tag{A.5}$$

$$\ln P_\omega^* = 37.04 - \frac{6276}{T + 273.15} - 3.416 \ln(T + 273.15) \tag{A.6}$$

$$m = \frac{W_t \left(183.1221 - 0.56845(T + 273.15) + 984.5679 e^{\frac{W_t}{115.96277}}\right)}{100 \times 56.105} \tag{A.7}$$

$$Y = 42.96 + 40.762T - 0.06682T^2 \tag{A.8}$$

$$\eta_v = \frac{U_{tn}}{U_{cell}} = \frac{\frac{\Delta H}{zF}}{U_{cell}} = \frac{3600 M_{\mathrm{H}_2} \cdot HHV}{zFU_{cell}} \tag{A.9}$$

Data availability

Data will be made available on request.

References

[1] International Energy Agency. CO2 emissions in 2022. 2023, http://dx.doi.org/10.1787/12ad1e1a-en.
[2] International Energy Agency . Renewables 2023. 2023, URL https://iea.blob.core.windows.net/assets/96d66a8b-d502-476b-ba94-54ffda84cf72/Renewables_2023.pdf.
[3] Dowling JA, Rinaldi KZ, Ruggles TH, Davis SJ, Yuan M, Tong F, et al. Role of long-duration energy storage in variable renewable electricity systems. Joule 2020;4(9):1907–28. http://dx.doi.org/10.1016/j.joule.2020.07.007.
[4] Bialek J. What does the GB power outage on 9 August 2019 tell us about the current state of decarbonised power systems? Energy Policy 2020;146:111821. http://dx.doi.org/10.1016/j.enpol.2020.111821.
[5] Breaking the hard-to-abate bottleneck in China’s path to carbon neutrality with clean hydrogen. Nat Energy 2022;7(10):955–65. http://dx.doi.org/10.1038/s41560-022-01114-6.
[6] Buttler A, Spliethoff H. Current status of water electrolysis for energy storage, grid balancing and sector coupling via power-to-gas and power-to-liquids: A review. Renew Sustain Energy Rev 2018;82(February 2017):2440–54. http://dx.doi.org/10.1016/j.rser.2017.09.003.
[7] Huang C. Analytical modeling and control of grid-scale alkaline electrolyzer plant for frequency support in wind-dominated electricity-hydrogen systems. IEEE Trans Sustain Energy 2023;14(1):217–32. http://dx.doi.org/10.1109/TSTE.2022.3208361.
[8] Hydrogen Council, McKinsey&Company. Hydrogen insights 2022: An updated perspective on hydrogen market development and actions required to unlock hydrogen at scale. In: Hydrogen council. Tech. rep., (September). 2022, URL www.hydrogencouncil.com.
[9] Chehade Z, Mansilla C, Lucchese P, Hilliard S, Proost J. Review and analysis of demonstration projects on power-to-X pathways in the world. Int J Hydrog Energy 2019;44(51):27637–55. http://dx.doi.org/10.1016/j.ijhydene.2019.08.260.
[10] Lange H, Klose A, Lippmann W, Urbas L. Technical evaluation of the flexibility of water electrolysis systems to increase energy flexibility: A review. Int J Hydrog Energy 2023;48(42):15771–83. http://dx.doi.org/10.1016/j.ijhydene.2023.01.044.
[11] Trattner A, Höglinger M, Macherhammer MG, Sartory M. Renewable hydrogen: Modular concepts from production over storage to the consumer. Chemie- Ingenieur- Tech 2021;93(4):706–16. http://dx.doi.org/10.1002/cite.202000197.
[12] Martinez Lopez VA, Ziar H, Haverkort JW, Zeman M, Isabella O. Dynamic operation of water electrolyzers: A review for applications in photovoltaic systems integration. Renew Sustain Energy Rev 2023;182(May):113407. http://dx.doi.org/10.1016/j.rser.2023.113407.
[13] Ji M, Wang J. Review and comparison of various hydrogen production methods based on costs and life cycle impact assessment indicators. Int J Hydrog Energy 2021;46(78):38612–35. http://dx.doi.org/10.1016/j.ijhydene.2021.09.142.
[14] Shen X, Zhang X, Li G, Lie TT, Hong L. Experimental study on the external electrical thermal and dynamic power characteristics of alkaline water electrolyzer. Int J Energy Res 2018;42(10):3244–57. http://dx.doi.org/10.1002/er.4076.
[15] Varela C, Mostafa M, Zondervan E. Modeling alkaline water electrolysis for power-to-x applications: A scheduling approach. Int J Hydrog Energy 2021;46(14):9303–13. http://dx.doi.org/10.1016/j.ijhydene.2020.12.111.
[16] Olivier P, Bourasseau C, Bouamama PB. Low-temperature electrolysis system modelling: A review. Renew Sustain Energy Rev 2017;78(May):280–300. http://dx.doi.org/10.1016/j.rser.2017.03.099.
[17] Hu S, Guo B, Ding S, Yang F, Dang J, Liu B, et al. A comprehensive review of alkaline water electrolysis mathematical modeling. Appl Energy 2022;327(September):120099. http://dx.doi.org/10.1016/j.apenergy.2022.120099.
[18] Daoudi C, Bounahmidi T. Overview of alkaline water electrolysis modeling. Int J Hydrog Energy 2024;49:646–67. http://dx.doi.org/10.1016/j.ijhydene.2023.08.345.

[19] Meng X, Jiang L, He M, Wang X, Liu J. A novel multi-scale frequency regulation method of hybrid rectifier and its specific application in electrolytic hydrogen production. IEEE Trans Power Electron 2023;38(1):123–9. http://dx.doi.org/10.1109/TPEL.2022.3207601.

[20] Guilbert D, Collura SM, Scipioni A. DC/DC converter topologies for electrolyzers: State-of-the-art and remaining key issues. Int J Hydrog Energy 2017;42(38):23966–85. http://dx.doi.org/10.1016/j.ijhydene.2017.07.174.

[21] Hammoudi M, Henao C, Agbossou K, Dubé Y, Doumbia ML. New multi-physics approach for modelling and design of alkaline electrolyzers. Int J Hydrog Energy 2012;37(19):13895–913. http://dx.doi.org/10.1016/j.ijhydene.2012.07.015.

[22] Henao C, Agbossou K, Hammoudi M, Dubé Y, Cardenas A. Simulation tool based on a physics model and an electrical analogy for an alkaline electrolyser. J Power Sources 2014;250:58–67. http://dx.doi.org/10.1016/j.jpowsour.2013.10.086.

[23] Ulleberg Ø. Modeling of advanced alkaline electrolyzers: A system simulation approach. Int J Hydrog Energy 2003;28(1):21–33. http://dx.doi.org/10.1016/S0360-3199(02)00033-2.

[24] Diéguez PM, Ursúa A, Sanchis P, Sopena C, Guelbenzu E, Gandía LM. Thermal performance of a commercial alkaline water electrolyzer: Experimental study and mathematical modeling. Int J Hydrog Energy 2008;33(24):7338–54. http://dx.doi.org/10.1016/j.ijhydene.2008.09.051.

[25] Qi R, Li J, Lin J, Song Y, Wang J, Cui Q, et al. Thermal modelling and controller design of an alkaline electrolysis system under dynamic operating conditions. Appl Energy 2022;332(October 2022):120551. http://dx.doi.org/10.1016/j.apenergy.2022.120551, arXiv:2202.13422. URL http://arxiv.org/abs/2202.13422.

[26] Kélouwani S, Agbossou K, Chahine R. Model for energy conversion in renewable energy system with hydrogen storage. J Power Sources 2005;140(2):392–9. http://dx.doi.org/10.1016/j.jpowsour.2004.08.019.

[27] Kim H, Park M, Lee KS. One-dimensional dynamic modeling of a high-pressure water electrolysis system for hydrogen production. Int J Hydrog Energy 2013;38(6):2596–609. http://dx.doi.org/10.1016/j.ijhydene.2012.12.006, URL https://www.sciencedirect.com/science/article/pii/S0360319912026444.

[28] Haug P, Kreitz B, Koj M, Turek T. Process modelling of an alkaline water electrolyzer. Int J Hydrog Energy 2017;42(24):15689–707. http://dx.doi.org/10.1016/j.ijhydene.2017.05.031.

[29] Sánchez M, Amores E, Rodríguez L, Clemente-Jul C. Semi-empirical model and experimental validation for the performance evaluation of a 15 kW alkaline water electrolyzer. Int J Hydrog Energy 2018;43(45):20332–45. http://dx.doi.org/10.1016/j.ijhydene.2018.09.029.

[30] Qi R, Gao X, Lin J, Song Y, Wang J, Qiu Y, et al. Pressure control strategy to extend the loading range of an alkaline electrolysis system. Int J Hydrog Energy 2021;46(73):35997–6011. http://dx.doi.org/10.1016/j.ijhydene.2021.08.069.

[31] Hug W, Bussmann H, Brinner A. Intermittent operation and operation modeling of an alkaline electrolyzer. Int J Hydrog Energy 1993;18(12):973–7. http://dx.doi.org/10.1016/0360-3199(93)90078-O.

[32] El-Askary WA, Sakr IM, Ibrahim KA, Balabel A. Hydrodynamics characteristics of hydrogen evolution process through electrolysis: Numerical and experimental studies. Energy 2015;90:722–37. http://dx.doi.org/10.1016/j.energy.2015.07.108.

[33] Fragiacomo P, Genovese M. Modeling and energy demand analysis of a scalable green hydrogen production system. Int J Hydrog Energy 2019;44(57):30237–55. http://dx.doi.org/10.1016/j.ijhydene.2019.09.186.

[34] Zarghami A, Deen NG, Vreman AW. CFD modeling of multiphase flow in an alkaline water electrolyzer. Chem Eng Sci 2020;227:115926. http://dx.doi.org/10.1016/j.ces.2020.115926.

[35] Mat MD, Aldas K, Ilegbusi OJ. A two-phase flow model for hydrogen evolution in an electrochemical cell. Int J Hydrog Energy 2004;29(10):1015–23. http://dx.doi.org/10.1016/j.ijhydene.2003.11.007.

[36] Aldas K, Pehlivanoglu N, Mat MD. Numerical and experimental investigation of two-phase flow in an electrochemical cell. Int J Hydrog Energy 2008;33(14):3668–75. http://dx.doi.org/10.1016/j.ijhydene.2008.04.047.

[37] Edgar TF, Hahn J. Process automation. In: Springer handbook of automation. Springer; 2009, p. 529–43.

[38] Kauranen PS, Lund PD, Vanhanen JP. Development of a self-sufficient solar - hydrogen energy system. 19, (1):1994, p. 99–106.

[39] Vanhanen JP, Kauranen PS, Lund PD, Manninen LM. Simulation of solar hydrogen energy systems. Sol Energy 1994;53(3):267–78. http://dx.doi.org/10.1016/0038-092X(94)90633-5.

[40] Rogers JA, Maznev AA, Banet MJ, Nelson KA. Optical generation and characterization of acoustic waves in thin films: Fundamentals and applications. In: Annual review of materials science, vol. 30, 2000, p. 117–57. http://dx.doi.org/10.1146/annurev.matsci.30.1.117.

[41] Busquet S, Hubert CE, Labbé J, Mayer D, Metkemeijer R. A new approach to empirical electrical modelling of a fuel cell, an electrolyser or a regenerative fuel cell. J Power Sources 2004;134(1):41–8. http://dx.doi.org/10.1016/j.jpowsour.2004.02.018.

[42] Vogt H, Balzer RJ. The bubble coverage of gas-evolving electrodes in stagnant electrolytes. Electrochim Acta 2005;50(10):2073–9. http://dx.doi.org/10.1016/j.electacta.2004.09.025.

[43] Roy A, Watson S, Infield D. Comparison of electrical energy efficiency of atmospheric and high-pressure electrolysers. Int J Hydrog Energy 2006;31(14):1964–79. http://dx.doi.org/10.1016/j.ijhydene.2006.01.018.

[44] Shen M, Bennett N, Ding Y, Scott K. A concise model for evaluating water electrolysis. Int J Hydrog Energy 2011;36(22):14335–41. http://dx.doi.org/10.1016/j.ijhydene.2010.12.029, URL http://dx.doi.org/10.1016/j.ijhydene.2010.12.029.

[45] Artuso P, Gammon R, Orecchini F, Watson SJ. Alkaline electrolysers: Model and real data analysis. Int J Hydrog Energy 2011;36(13):7956–62. http://dx.doi.org/10.1016/j.ijhydene.2011.01.094, URL http://dx.doi.org/10.1016/j.ijhydene.2011.01.094.

[46] Ursúa A, Sanchis P. Static-dynamic modelling of the electrical behaviour of a commercial advanced alkaline water electrolyser. Int J Hydrog Energy 2012;37(24):18598–614. http://dx.doi.org/10.1016/j.ijhydene.2012.09.125.

[47] Milewski J, Guandalini G, Campanari S. Modeling an alkaline electrolysis cell through reduced-order and loss-estimate approaches. J Power Sources 2014;269:203–11. http://dx.doi.org/10.1016/j.jpowsour.2014.06.138.

[48] Amores E, Rodríguez J, Carreras C. Influence of operation parameters in the modeling of alkaline water electrolyzers for hydrogen production. Int J Hydrog Energy 2014;39(25):13063–78. http://dx.doi.org/10.1016/j.ijhydene.2014.07.001.

[49] Abdin Z, Webb CJ, Gray EMA. Modelling and simulation of an alkaline electrolyser cell. Energy 2017;138:316–31. http://dx.doi.org/10.1016/j.energy.2017.07.053.

[50] Rodríguez J, Palmas S, Sánchez-Molina M, Amores E, Mais L, Campana R. Simple and precise approach for determination of Ohmic contribution of diaphragms in alkaline water electrolysis. Membranes 2019;9(10). http://dx.doi.org/10.3390/membranes9100129.

[51] Jang D, Cho HS, Kang S. Numerical modeling and analysis of the effect of pressure on the performance of an alkaline water electrolysis system. Appl Energy 2021;287(January):116554. http://dx.doi.org/10.1016/j.apenergy.2021.116554.

[52] Jang D, Choi W, Cho HS, Cho WC, Kim CH, Kang S. Numerical modeling and analysis of the temperature effect on the performance of an alkaline water electrolysis system. J Power Sources 2021;506(May):230106. http://dx.doi.org/10.1016/j.jpowsour.2021.230106.

[53] Hodges A, Hoang AL, Tsekouras G, Wagner K, Lee CY, Swiegers GF, et al. A high-performance capillary-fed electrolysis cell promises more cost-competitive renewable hydrogen. Nat Commun 2022;13(1):1–11. http://dx.doi.org/10.1038/s41467-022-28953-x.

[54] Haug P, Koj M, Turek T. Influence of process conditions on gas purity in alkaline water electrolysis. Int J Hydrog Energy 2017;42(15):9406–18. http://dx.doi.org/10.1016/j.ijhydene.2016.12.111, URL http://dx.doi.org/10.1016/j.ijhydene.2016.12.111.

[55] Kirati SK, Hammoudi M, Mousli IM. Hybrid energy system for hydrogen production in the Adrar region (Algeria): Production rate and purity level. Int J Hydrog Energy 2018;43(6):3378–93. http://dx.doi.org/10.1016/j.ijhydene.2017.09.083.

[56] Haug P. Experimental and theoretical investigation of gas purity in alkaline water electrolysis. 2019, p. 155.

[57] Rizwan M, Alstad V, Jäschke J. Design considerations for industrial water electrolyzer plants. Int J Hydrog Energy 2021;46(75):37120–36. http://dx.doi.org/10.1016/j.ijhydene.2021.09.018.

[58] Dynamic energy and mass balance model for an industrial alkaline water electrolyzer plant process. Int J Hydrog Energy 2022;47(7):4328–45. http://dx.doi.org/10.1016/j.ijhydene.2021.11.126.

[59] Aldas K. Application of a two-phase flow model for hydrogen evolution in an electrochemical cell. Appl Math Comput 2004;154(2):507–19. http://dx.doi.org/10.1016/S0096-3003(03)00731-8.

[60] Philippe M, Jérôme H, Sebastien B, Gérard P. Modelling and calculation of the current density distribution evolution at vertical gas-evolving electrodes. Electrochim Acta 2005;51(6):1140–56. http://dx.doi.org/10.1016/j.electacta.2005.06.007.

[61] Rodríguez J, Amores E. Cfd modeling and experimental validation of an alkaline water electrolysis cell for hydrogen production. Processes 2020;8(12):1–17. http://dx.doi.org/10.3390/pr8121634.

[62] Le Bideau D, Mandin P, Benbouzid M, Kim M, Sellier M, Ganci F, et al. Eulerian two-fluid model of alkaline water electrolysis for hydrogen production. Energies 2020;13(13):1–14. http://dx.doi.org/10.3390/en13133394.

[63] Lee J, Alam A, Park C, Yoon S, Ju H. Modeling of gas evolution processes in porous electrodes of zero-gap alkaline water electrolysis cells. Fuel 2022;315(November 2021):123273. http://dx.doi.org/10.1016/j.fuel.2022.123273.

[64] Korp M. Operation planning of hydrogen storage connected to wind power operating in a power market. IEEE Trans Energy Convers 2006;21(3):742–9.

[65] Hajimiragha AH, Zadeh MRD, Moazeni S. Microgrids frequency control considerations within the framework of the optimal generation scheduling problem. IEEE Trans Smart Grid 2015;6(2):534–47. http://dx.doi.org/10.1109/TSG.2014.2375251.

[66] Won W, Kwon H, Han J-h, Kim J. Design and operation of renewable energy sources based hydrogen supply system : Technology integration and optimization. Renew Energy 2017;103:226–38. http://dx.doi.org/10.1016/j.renene.2016.11.038.
[67] Jaramillo LB, Weidlich A. Optimal microgrid scheduling with peak load reduction involving an electrolyzer and flexible loads. 169, 2016, p. 857–65. http://dx.doi.org/10.1016/j.apenergy.2016.02.096.
[68] El-taweel NA, Member S, Khani H, Farag HEZ, Member S. Hydrogen storage optimal scheduling for fuel supply and capacity-based demand response program under dynamic hydrogen pricing. IEEE Trans Smart Grid 2019;10(4):4531–42. http://dx.doi.org/10.1109/TSG.2018.2863247.
[69] Zhao Y, Chen C, Teng M, Zhong J, Sun X. Refined modeling and approximated aggregation method for alkaline water electrolyzers in power system optimal scheduling. Int J Hydrog Energy 2024;52(PA):200–12. http://dx.doi.org/10.1016/j.ijhydene.2023.11.204.
[70] Zheng Y, Huang C, You S, Zong Y. Economic evaluation of a power-to-hydrogen system providing frequency regulation reserves: a case study of Denmark. Int J Hydrog Energy 2023;48(67):26046–57. http://dx.doi.org/10.1016/j.ijhydene.2023.03.253.
[71] Tebibel H. Methodology for multi-objective optimization of wind turbine/battery/electrolyzer system for decentralized clean hydrogen production using an adapted power management strategy for low wind speed conditions. Energy Convers Manage 2021;238:114125. http://dx.doi.org/10.1016/j.enconman.2021.114125.
[72] Alonso AM, Matute G, Yusta JM, Coosemans T. Multi-state optimal power dispatch model for power-to-power systems in off-grid hybrid energy systems : A case study in Spain. Int J Hydrog Energy 2023;52:1045–61. http://dx.doi.org/10.1016/j.ijhydene.2023.06.019.
[73] Zhang W, Maleki A, Rosen MA, Liu J. Optimization with a simulated annealing algorithm of a hybrid system for renewable energy including battery and hydrogen storage. Energy 2018;163:191–207. http://dx.doi.org/10.1016/j.energy.2018.08.112.
[74] Gurobi Optimization, LLC. Gurobi optimizer reference manual. 2021, URL https://www.gurobi.com.
[75] Li B, Roche R, Miraoui A. Microgrid sizing with combined evolutionary algorithm and MILP unit commitment. Appl Energy 2017;188:547–62. http://dx.doi.org/10.1016/j.apenergy.2016.12.038.
[76] Li B, Roche R, Paire D, Miraoui A. Sizing of a stand-alone microgrid considering electric power, cooling/heating, hydrogen loads and hydrogen storage degradation. Applied Energy 2017;205:1244–59. http://dx.doi.org/10.1016/j.apenergy.2017.08.142.
[77] Behzadi MS, Niasati M. Comparative performance analysis of a hybrid PV/FC/battery stand-alone system using different power management strategies and sizing approaches. Int J Hydrog Energy 2015;40(1):538–48. http://dx.doi.org/10.1016/j.ijhydene.2014.10.097.
[78] Dufo-López R, Bernal-Agustín JL. Multi-objective design of PV-wind-diesel-hydrogen-battery systems. Renew Energy 2008;33(12):2559–72. http://dx.doi.org/10.1016/j.renene.2008.02.027.
[79] Zheng Y, Huang C, Tan J, You S, Zong Y, Træholt C. Off-grid wind/hydrogen systems with multi-electrolyzers: Optimized operational strategies. Energy Convers Manage 2023;295(May):117622. http://dx.doi.org/10.1016/j.enconman.2023.117622.
[80] Zheng Y, Wang J, You S, Li X, Bindner HW, Münster M. Data-driven scheme for optimal day-ahead operation of a wind/hydrogen system under multiple uncertainties. Appl Energy 2023;329(October 2022):120201. http://dx.doi.org/10.1016/j.apenergy.2022.120201.
[81] Raheli E, Werner Y, Kazempour J. A conic model for electrolyzer scheduling. Comput Chem Eng 2023;179(July):0–11. http://dx.doi.org/10.1016/j.compchemeng.2023.108450, arXiv:2306.10951.
[82] Zheng Y, You S, Bindner HW, Marie M. Incorporating optimal operation strategies into investment planning for wind / electrolyser system. CSEE J Power Energy Syst 2022;8(2):347–59. http://dx.doi.org/10.17775/CSEEJPES.2021.04240.
[83] Cheng X, Lin J, Liu F, Qiu Y, Song Y, Li J, et al. A coordinated frequency regulation and bidding method for wind-electrolysis joint systems. IEEE Trans Sustain Energy 2023;14(3):1370–84. http://dx.doi.org/10.1109/TSTE.2022.3233062.
[84] Li J, Lin J, Song Y, Xiao J. Coordinated planning of HVDCs and power-to-hydrogen supply chains for interregional renewable energy utilization. IEEE Trans Sustain Energy 2022;13(4):1913–29.
[85] Marocco P, Ferrero D, Lanzini A, Santarelli M. Optimal design of stand-alone solutions based on RES + hydrogen storage feeding off-grid communities. Energy Convers Manage 2021;238:114147. http://dx.doi.org/10.1016/j.enconman.2021.114147.
[86] Cau G, Cocco D, Petrollese M, Knudsen Kær S, Milan C. Energy management strategy based on short-term generation scheduling for a renewable microgrid using a hydrogen storage system. Energy Convers Manage 2014;87:820–31. http://dx.doi.org/10.1016/j.enconman.2014.07.078.
[87] Eriksson EL, Gray EMA. Optimization of renewable hybrid energy systems – a multi-objective approach. Renew Energy 2019;133:971–99. http://dx.doi.org/10.1016/j.renene.2018.10.053.
[88] Huang C, Zong Y, You S, Træholt C, Zheng Y, Wang J. Economic and resilient operation of hydrogen-based microgrids : An improved MPC-based optimal scheduling scheme considering security constraints of hydrogen facilities. Appl Energy 2023;335(January):120762. http://dx.doi.org/10.1016/j.apenergy.2023.120762.
[89] Huang C, Zong Y, You S, Træholt C. Economic model predictive control for multi-energy system considering hydrogen-thermal-electric dynamics and waste heat recovery of MW-level alkaline electrolyzer. Energy Convers Manage 2022;265:115697. http://dx.doi.org/10.1016/J.ENCONMAN.2022.115697.
[90] Hu Q, Lin J, Zeng Q, Fu C, Li J. Optimal control of a hydrogen microgrid based on an experiment validated P2HH model. (iii). 2019, http://dx.doi.org/10.1049/iet-rpg.2019.0544.
[91] Ge P, Hu Q, Wu Q, Dou X, Wu Z, Ding Y. Increasing operational flexibility of integrated energy systems by introducing power to hydrogen. 14, 2020, p. 372–80. http://dx.doi.org/10.1049/iet-rpg.2019.0663.
[92] Pan G, Member S, Gu W, Member S, Lu Y, Member S. Optimal planning for electricity-hydrogen integrated energy system considering power to hydrogen and heat and seasonal storage. IEEE Trans Sustain Energy 2020;11(4):2662–76. http://dx.doi.org/10.1109/TSTE.2020.2970078.
[93] Zheng Y, You S, Bindner HW, Münster M. Optimal day-ahead dispatch of an alkaline electrolyser system concerning thermal – electric properties and state-transitional dynamics. Appl Energy 2022;307:118091. http://dx.doi.org/10.1016/j.apenergy.2021.118091.
[94] Li J, Lin J, Song Y, Xing X, Fu C. Operation optimization of power to hydrogen and heat (P2HH) in ADN coordinated with the district heating network. IEEE Trans Sustain Energy 2019;10(4):1672–83. http://dx.doi.org/10.1109/TSTE.2018.2868827.
[95] Qiu Y, Zhou B, Zang T, Zhou Y, Chen S, Qi R, et al. Extended load flexibility of utility-scale P2H plants : Optimal production scheduling considering dynamic thermal and HTO impurity effects. Renew Energy 2023;217(July):119198. http://dx.doi.org/10.1016/j.renene.2023.119198.
[96] Khaligh V, Ghezelbash A, Zarei M, Liu J, Won W. Efficient integration of alkaline water electrolyzer – a model predictive control approach for a sustainable low-carbon district heating system. Energy Convers Manage 2023;292(July):117404. http://dx.doi.org/10.1016/j.enconman.2023.117404.
[97] Hong Z, Wei Z, Han X. Optimization scheduling control strategy of wind-hydrogen system considering hydrogen production efficiency. J Energy Storage 2022;47(April 2021):103609. http://dx.doi.org/10.1016/j.est.2021.103609.
[98] Yang Y, La BD, Stewart K, Lair L, Phan NL, Das R, et al. The scheduling of alkaline water electrolysis for hydrogen production using hybrid energy sources. Energy Convers Manage 2022;257:115408. http://dx.doi.org/10.1016/j.enconman.2022.115408.
[99] Liang T, Chai L, Cao X, Tan J, Jing Y, Lv L. Real-time optimization of large-scale hydrogen production systems using off-grid renewable energy : Scheduling strategy based on deep reinforcement learning. Renew Energy 2024;224(August 2023):120177. http://dx.doi.org/10.1016/j.renene.2024.120177.
[100] Konstantinopoulos SA, Anastasiadis AG, Vokas GA, Kondylis GP, Polyzakis A. ScienceDirect optimal management of hydrogen storage in stochastic smart microgrid operation. Int J Hydrog Energy 2017;43(1):490–9. http://dx.doi.org/10.1016/j.ijhydene.2017.06.116.
[101] Huang W, Zhang B, Ge L, He J, Liao W, Ma P. Day-ahead optimal scheduling strategy for electrolytic water to hydrogen production in zero-carbon parks type microgrid for optimal utilization of electrolyzer. J Energy Storage 2023;68(March):107653. http://dx.doi.org/10.1016/j.est.2023.107653.
[102] Veerakumar N, Ahmad Z, Adabi ME, Torres JR, Palensky P, Van Der Meijden M, et al. Fast active power-frequency support methods by large scale electrolyzers for multi-energy systems. IEEE PES Innov Smart Grid Technol Conf Eur 2020;2020-October:151–5. http://dx.doi.org/10.1109/ISGT-Europe47291.2020.9248949.
[103] Kiaee M, Cruden A, Infield D, Chladek P. Utilisation of alkaline electrolysers to improve power system frequency stability with a high penetration of wind power. IET Renew Power Gener 2014;8(5):529–36. http://dx.doi.org/10.1049/iet-rpg.2012.0190.
[104] Matute G, Yusta JM, Correas LC. ScienceDirect techno-economic modelling of water electrolysers in the range of several MW to provide grid services while generating hydrogen for different applications : A case study in Spain applied to mobility with FCEVs. Int J Hydrog Energy 2019;44(33):17431–42. http://dx.doi.org/10.1016/j.ijhydene.2019.05.092.
[105] Grueger F, Möhrke F, Robinius M, Stolten D. Early power to gas applications : Reducing wind farm forecast errors and providing secondary control reserve. Appl Energy 2017;192:551–62. http://dx.doi.org/10.1016/j.apenergy.2016.06.131.
[106] Maluenda M, Córdova S, Lorca Á, Negrete-pincetic M. Optimal operation scheduling of a PV-BESS-electrolyzer system for hydrogen production and frequency regulation. Appl Energy 2023;344(November 2022):121243. http://dx.doi.org/10.1016/j.apenergy.2023.121243.
[107] Attemene NS, Agbli KS, Fofana S, Hissel D. ScienceDirect optimal sizing of a wind , fuel cell , electrolyzer , battery and supercapacitor system for off-grid applications. Int J Hydrog Energy 2019;45(8):5512–25. http://dx.doi.org/10.1016/j.ijhydene.2019.05.212.

[108] Yu Z, Member S, Lin J, Liu F, Member S. Optimal sizing and pricing of grid-connected renewable power to ammonia systems considering the limited flexibility of ammonia synthesis. IEEE Trans Power Syst 2024;39(2):3631–48. http://dx.doi.org/10.1109/TPWRS.2023.3279130.

[109] Angélica M, Gabriel J, Clúa G. Sizing and analytical optimization of an alkaline water electrolyzer powered by a grid-assisted wind turbine to minimize grid power exchange. Renew Energy 2023;216(July):118990. http://dx.doi.org/10.1016/j.renene.2023.118990.

[110] Ma Z, Tian T, Cui Q, Shu J, Zhao J. ScienceDirect rapid sizing of a hydrogen-battery storage for an offshore wind farm using convex programming. Int J Hydrog Energy 2023;48(58):21946–58. http://dx.doi.org/10.1016/j.ijhydene.2023.03.037.

[111] Khalilnejad A, Riahy GH. A hybrid wind-PV system performance investigation for the purpose of maximum hydrogen production and storage using advanced alkaline electrolyzer. Energy Convers Manage 2014;80:398–406. http://dx.doi.org/10.1016/j.enconman.2014.01.040.